NASA TN D-1937

60p.

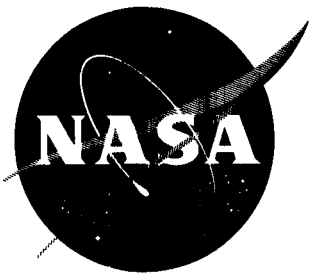

TECHNICAL NOTE

D-1937

LOW-SPEED INVESTIGATION OF CABLE TENSION AND AERODYNAMIC CHARACTERISTICS OF A PARAWING AND SPACECRAFT COMBINATION

By William C. Sleeman, Jr.

Langley Research Center
Langley Station, Hampton, Va.

NATIONAL AERONAUTICS AND SPACE ADMINISTRATION
WASHINGTON
July 1963

NATIONAL AERONAUTICS AND SPACE ADMINISTRATION

TECHNICAL NOTE D-1937

LOW-SPEED INVESTIGATION OF CABLE TENSION AND AERODYNAMIC CHARACTERISTICS OF A PARAWING AND SPACECRAFT COMBINATION

By William C. Sleeman, Jr.

SUMMARY

A low-speed investigation was made to obtain detailed information on longitudinal aerodynamic characteristics and cable tension loads for a parawing and spacecraft configuration. The 55° swept parawing represented an inflated-tube structure capable of being packaged in the spacecraft and of being deployed for glide and flared landing recovery of the spacecraft. Three basic cable riggings were studied in order to simulate a glide configuration, a dive configuration, and a landing configuration. Tests were conducted over a range of dynamic pressures from 4 to 14 pounds per square foot for the glide and flare configurations at the design angle of attack for each configuration. Tests were also made over an angle-of-attack range above and below the design condition for all the configurations. Some of the tests were repeated with the model in an inverted position in order to investigate effects of wing weight.

The maximum lift-drag ratio for the complete model was 2.7 and for the wing alone was 3.5. The longitudinal stability for the glide and flare configurations was high at angles of attack near the design angle for each configuration. For angles of attack somewhat below the design point, the diagonal cable became slack and the stability was about neutral. The cable-tension data for the design conditions indicated that approximately half of the total tension in all cables was carried in the cables going to the leading edge and the remaining half was carried in the three cables going to the center keel.

Even though there are a number of possible limitations to the applicability of the present data, it is believed that the results obtained provide valuable information on rigging condition for stability and trim and give a good indication of the distribution of cable loads for the type of configuration investigated.

INTRODUCTION

A considerable amount of aerodynamic information has been obtained on parawings alone and some results are available for parawings in combination with

different types of payloads. Results of some of these studies are presented in references 1 to 9. The available information on wing-alone aerodynamic characteristics may be used to determine configuration arrangements which provide stability and trim for given conditions and to obtain a first-order indication of the cable-load distribution for cable-supported payloads. Determination of cable loads from wing-alone data may be subject to inaccuracies because some cable arrangements may be statically indeterminate and estimations of the distribution of cable loads would require assumptions that may be subject to appreciable inaccuracies. The possible uncertainties in estimating cable loads indicated a need for an experimental investigation of these loads for a parawing configuration.

The present investigation was undertaken to provide detailed information on the cable tension loads for a parawing and spacecraft combination. The wing of the model was swept 55° and had rigid-tube leading edges and keel, with a rigid spreader bar between the keel and each leading edge. The wing keel was connected to the spacecraft by three cables: a front cable, a diagonal cable, and a rear cable. The lengths of these cables determined the angle of the wing and the location of the wing with respect to the spacecraft. A single cable went to each leading edge of the wing from the side of the spacecraft. The wing surface was composed of a flexible membrane attached to the leading edges and keel and had a flat planform sweep of 45°. Three basic cable riggings were studied in this investigation in order to simulate a glide configuration, a flare configuration, and a dive configuration.

The present investigation required some different experimental techniques than had previously been used and a significant part of the investigation was therefore concerned with evaluating the test technique. Most of the model configurations in this phase of the investigation were tested in an upright and inverted position through an angle-of-attack range and were tested over a range of dynamic pressures at given angles of attack. Measurements of cable tension loads were made with tension gages in each cable and the overall aerodynamic characteristics of the wing and spacecraft were determined from measurements obtained from a six-component strain-gage balance inside the spacecraft.

A boltrope was installed in the trailing edge of the wing in order to minimize trailing-edge flutter at low angles of attack. Test results were obtained with the boltrope slack and with the boltrope shortened 4 percent of the trailing-edge length. Aerodynamic characteristics of the wing alone were obtained with the wing mounted directly on a six-component balance and aerodynamic characteristics in pitch of the spacecraft alone were also determined.

COEFFICIENTS AND SYMBOLS

The data presented in this report are referred to the axis system shown in figure 1. The moment reference for the data obtained on the wing-alone configuration was located at 50 percent of the keel length and on the center line of the keel. The moment reference for the complete configuration and the spacecraft alone was located in the spacecraft as shown in figure 2.

Coefficients and symbols used in the presentation of data are as follows:

C_L lift coefficient, $\frac{\text{Lift}}{qS}$

C_D drag coefficient, $\frac{\text{Drag}}{qS}$

C_m pitching-moment coefficient, $\frac{\text{Pitching moment}}{qSl_k}$

C_N normal-force coefficient, $\frac{\text{Normal force}}{qS}$

C_A axial-force coefficient, $\frac{\text{Axial force}}{qS}$

C_T cable-tension coefficient, $\frac{\text{Cable tension}}{qS}$

$C_{T,Y}$ lateral component of cable-tension coefficient, considered positive for left line, $C_T \cos \phi$

l_k length of wing keel from apex at intersection of leading-edge center lines to rear of constant diameter section of keel, ft

q free-stream dynamic pressure, lb/sq ft

S flat planform area of wing canopy, sq ft

$\overline{X}$ longitudinal distance along wing keel from wing apex to line normal to keel and passing through moment reference for complete model, expressed in terms of keel length

$\overline{Z}$ distance of wing-keel center line from moment reference for complete model, measured normal to the wing keel and expressed in terms of keel length

x_{cp} longitudinal position of center of pressure, expressed in terms of keel length, $0.50 - \frac{C_m}{C_N}$

L/D lift-drag ratio, C_L/C_D

α angle of attack of spacecraft center line, deg

α_k angle of attack of wing-keel center line, deg

γ inclination of wing-keel center line with respect to balance center line, deg

θ angle between support cables and wing keel when viewed from side, deg

ϕ angle between leading-edge cables and plane defined by center lines of wing leading edges and keel when viewed from rear and normal to plane containing leading-edge cables, deg

Designation of cables:

F front line from spacecraft to wing keel

B rear line from spacecraft to wing keel

D diagonal line from spacecraft to wing keel

L left line from spacecraft to left wing leading edge

R right line from spacecraft to right wing leading edge

MODEL DESCRIPTION

The general arrangement of the model tested is shown in figure 2. A photograph of the model is shown as figure 3. The spacecraft was made of wood and was attached to a six-component internal strain-gage balance mounted on a sting support. The structural members of the wing were made of soft balsa and were hollow except near the apex and cable attachment points. The leading edges and keel were reinforced with inset mahogany blocks at each cable attachment point, at the apex, and at junctures with the spreader bar.

The wing leading edges and keel had a relatively large diameter (7 percent of the keel length) in order to represent the size of an inflatable parawing designed for stowage in the spacecraft for use as a recovery device. The wing leading edges were hinged at the apex and at the juncture of the spreader bar and keel as shown in figure 2. The leading edges were hinged in order to measure the cable tension in such a manner that the results would be applicable to an inflated-tube structure which furnished no moment restraint at these points.

The wing canopy was made of ripstop nylon weighing 1.1 ounce per square yard laminated to 1/4-mil-thick Mylar with a minimum amount of adhesive. The canopy fabric weave was oriented with the warp running parallel to the trailing edge. The canopy was attached to the keel by a narrow aluminum strip (3/8 inch wide and 1/16 inch thick) along the top of the keel and was attached to the leading edges by wrapping the canopy around the outside of the leading edge as shown in figure 2. A boltrope of 1/32-inch-diameter stranded steel cable was installed in the fabric hem at the trailing edge of the canopy for all tests of the model and data were obtained for two boltrope conditions. Tests of the model with 4-percent boltrope were made with the boltrope length 96 percent of the flat-planform trailing-edge length.

The wing was attached to the spacecraft by 1/32-inch-diameter stranded steel cables and tension gages were installed in each cable just above the spacecraft attachments. The tension gages were attached to the spacecraft by means of a hook and swivel. Standard fishing-line swivels were installed below the wing attachment points, above and below each tension gage. All hooks and swivels were preloaded before installation on the model in order to check their strength and to eliminate changes in length due to loading during the tests.

The weight of the wing with all of the cables and swivels above the tension gages was 1,053 grams (2.32 pounds). The mass center of gravity of the wing alone was located approximately 13.8 inches aft of the wing apex.

The rigging conditions were selected for the model for three flight conditions. The glide configuration was selected for free glide near the lift coefficient for maximum lift-drag ratio. The cable lengths were selected to provide an angle of attack of 35° for the wing when the spacecraft was at an angle of attack of 17°, an increment in angle between the spacecraft and wing of 18°. The dive configuration was selected to allow the configuration to perform a preflare maneuver to gain speed before initiating the final flare for landing. To change from the glide to the dive configuration, the wing angle of attack was reduced from 35° to 20° and the spacecraft angle of attack reduced to 0°. The flare configuration was selected to provide a high lift coefficient by increasing the wing angle of attack to 45° and moving the configuration center of gravity rearward relative to the wing. Inasmuch as landing for this configuration would possibly be on skids with the spacecraft center line approximately horizontal, the spacecraft angle for the flare configuration was 0°.

The pitching-moment results of this investigation were referred to a moment reference which was located at a fixed point in the spacecraft. It should be pointed out that the center of gravity for the complete configuration would move somewhat when the wing position changed with respect to the spacecraft. The amount of this movement would, of course, depend upon the relative mass of the wing and spacecraft and upon the displacement of the wing from its basic location.

The rigging for the model was determined for a given configuration by computing the lengths of the keel lines required to locate the wing at the desired position and angle of attack with respect to the spacecraft, and the computed lengths were set on the model. The leading-edge lines were attached and adjusted to allow the leading edges to lie in the same plane as the keel at 0° bank angle. The lengths of the leading-edge lines were then obtained from measurements of the lines with trammel points. The cable lengths used in this investigation are given in table I.

TESTS AND CORRECTIONS

The present investigation was conducted in the Langley high-speed 7- by 10-foot tunnel which operates at atmospheric stagnation pressure. The tests were conducted over a range of dynamic pressures which varied from 4 to 14 pounds per square foot. Data were obtained for each configuration over the test range of

dynamic pressure at the design angle of attack for the particular configuration. In order to extend the usefulness of the data and to obtain stability and trim data, tests were conducted over an angle-of-attack range, generally at a dynamic pressure of 12 pounds per square foot.

Forces and moments acting on the complete configuration were measured by means of a six-component internal strain-gage balance. This balance was attached to the spacecraft and to a variable-angle sting-support system in which the angle of attack was controlled remotely over a range of approximately 24°. Tension in the support cables between the wing and spacecraft was measured with tension gages in each cable. Most of the investigation was made with the model in both an upright and inverted position in order to check possible effects of the direction in which the wing weight acted in relation to the spacecraft. For tests of the upright model, wind-off zeros were obtained with no load on the tension gages and only the weight of the spacecraft and tension gages acting on the six-component balance. The actual wing lift was therefore greater than the measured lift by the amount of the wing weight. The wind-off zeros for the tests with the model inverted were obtained for both the tension gages and the six-component balance supporting the weight of the wing and therefore the actual wing lift was measured in these tests. In addition to the force and moment data obtained in this investigation, photographs of the model were obtained for each test point in order to determine the angles of the lines and of the wing. Photographs of the model from the side were obtained with a remotely operated camera outside the tunnel and photographs of the model from the rear were obtained with a camera attached to the sting.

No blockage corrections or jet-boundary corrections to angle of attack or drag coefficients have been applied to the data inasmuch as these corrections are believed to be small for the present perforated slot configuration used in the Langley high-speed 7- by 10-foot tunnel. No corrections have been made for sting-support tares inasmuch as the tare effects on the cable loads would be very small.

PRESENTATION OF RESULTS

The basic results of this investigation were obtained with the model upright and are presented to show the effects of boltrope length for each configuration. The force and moment data for the complete configuration are presented with the cable-loads data, the cable angles, and wing position. Results of this investigation are presented in the following figures:

DISCUSSION

Basic Model

The maximum lift-drag ratio obtained for both the glide and flare configurations was about 2.7 and for the dive configuration was about 2.4. (See figs. 6 to 8.) These values of maximum lift-drag ratio appear somewhat lower than might be expected; however, they are consistent with the relatively low value of 3.5 obtained for the wing alone. Maximum lift-drag ratios obtained in a systematic wing planform study indicate that a value of at least 4.5 would be expected for a parawing with a 55° sweep and a 45° flat planform sweep. This systematic planform investigation was obtained on wings having small leading-edge diameters whereas the wing of the present model had a fairly large leading-edge diameter. It is believed, therefore, that the large diameter for the leading edges and the keel of the present wing were primarily responsible for the relatively low values of maximum lift-drag ratio obtained for the complete model configuration. Another factor that may be of importance with regard to the measured lift-drag ratios is the usual effect of model scale and test Reynolds number; however, there are no test results currently available for wings having large leading-edge diameters to indicate the magnitude of these effects.

Test results on the distribution of cable tension in the five lines connecting the wing and spacecraft, for the design conditions, indicated that approximately 25 percent of the total tension in all lines was carried in each of the two leading-edge cables. The remaining approximately 50 percent of the total cable tension was carried in the lines to the keel, with the diagonal line carrying somewhat higher tension than the front and rear lines.

For angles of attack considerably below the design angle, the diagonal cable was slack and the tension measured in all the lines was relatively invariant up to about 6° below the design angle. At this point the diagonal cable began to carry load and the tension in this line increased appreciably with angle of attack and the line carried approximately 30 percent of the total cable tension

at the highest test angle of attack. In like manner the tension in the front and rear lines began to decrease, and at the highest angle they carried approximately 8 and 12 percent of the total tension, respectively.

The lift and drag characteristics for the glide and flare configurations (figs. 6 and 7) showed a fairly smooth variation with angle of attack over the test range. The pitching-moment characteristics indicated a large amount of longitudinal stability near the design angle of attack for both the glide and flare configurations; however, longitudinal trim was not obtained at the design point. The trim characteristics will be discussed in connection with effects of boltrope length inasmuch as the boltrope length had a significant effect on longitudinal trim. Of perhaps more importance to the aerodynamic characteristics indicated by the test data is the abrupt break in the pitching-moment curves when going from moderate to high lift. If these characteristics are indicative of flight characteristics, the large loss of stability below the design angle of attack would be highly undesirable inasmuch as the configuration was either neutrally stable or slightly unstable and the pitching moments were near zero in the low angle-of-attack range. A configuration having these characteristics might be expected to have a pitch-down of the wing after a negative angle-of-attack excursion below the trim angle which could cause the wing to unload and to luff if the excursion was sufficiently large. The reason for the abrupt break in the pitching-moment curves can be seen from the cable-tension coefficients also presented in figures 6 to 8. The break in the pitching-moment curves corresponds directly to the diagonal line becoming slack (zero tension) as the angle of attack was decreased.

Effects of Boltrope Condition

Experience with testing parawings has indicated the desirability, in many cases, of placing a boltrope in the wing trailing edge in order to decrease trailing-edge flutter at low angles of attack. The use of considerable boltrope shortening has been found imperative on aeroelastic models simulating inflated-tube configurations in order to prevent trailing-edge flutter from ripping the canopy apart. A trailing-edge boltrope was accordingly installed on the present model and two boltrope conditions were investigated. The basic condition was taken as the 4-percent boltrope in which the length of the boltrope was 96 percent of the actual wing trailing-edge length (4 percent shortening of the boltrope). Results were also obtained for a slack boltrope condition in which the boltrope was in the trailing edge but was not attached at the ends.

The effects of boltrope length have been studied in a number of investigations and have been found to be fairly consistent for a range of wing configurations. Shortening of the boltrope by as much as 7 or 8 percent has been found to cause proportional increases in lift, drag, and negative pitching-moment increments with little stability change and had a fairly small effect on lift-drag ratio at a given lift coefficient. In these respects, the present data with 4-percent boltrope are consistent with data from past investigations. (See figs. 4 to 8.)

Comparison of cable-tension coefficients for the two boltrope conditions generally indicated effects that would be expected from the increased lift at a given angle of attack that accompanied shortening of the boltrope, that is, the cable tension which occurred with the 4-percent boltrope was greater than that for the slack boltrope condition. The exception to this general observation is the cable tension measured in the front line at the keel for which the tension coefficients were, for the most part, lower with the 4-percent boltrope than with the boltrope slack. This effect on the front line is probably due to the fact that shortening the boltrope caused an appreciable nose-down pitching moment which would be expected to relieve the tension in the front line. There were no large changes in measured wing angle of attack with differences in boltrope; however, the wing appeared to fly at a slightly higher angle of attack with the boltrope slack for spacecraft angles at which the diagonal cable was unloaded. (See figs. 6 and 7.)

The effects of boltrope condition were somewhat different for the dive configuration than for the glide and flare configurations. The longitudinal aerodynamic characteristics presented in figure 8 indicate that the effects of boltrope conditions are reversed for the transition from low to moderate angles of attack for the dive configuration. In like manner, the longitudinal and vertical position of the wing ($\bar{X}$ and $\bar{Z}$ in fig. 8) varied greatly over the angle-of-attack range with the boltrope slack for the dive configuration whereas very little effect of boltrope was noted on these factors for the other configurations and there was a comparatively small variation with angle of attack. The dive configuration was very difficult to test either in an upright or an inverted position because the diagonal line tended to become slack at low angles of attack and the front line became slack at high angles. This difficulty in flying the wing for the dive configuration was also aggravated by the low design angle of attack of the wing ($\alpha_k = 20^\circ$) and data could not be obtained with the boltrope slack at dynamic pressures less than 14 pounds per square foot.

Initial attempts to test the model with the wing in a position rearward of the one used in obtaining the present results were unsuccessful because the rigging would not allow the wing to assume an angle of attack large enough to load the wing so that it would even support the wing weight, regardless of the spacecraft angle of attack. It appeared from these tests that possibly the resultant force vector on the wing was acting so far back with respect to the spacecraft attachment points that the wing angle of attack could not be increased by increasing the spacecraft angle of attack. The fact that the wing could be flown in the more forward position of the present tests appears to substantiate this assumption.

The difficulties encountered in testing the present dive configuration indicate that the particular rigging used would probably not be satisfactory for a flight vehicle inasmuch as the low design angle of attack and the tendency of the front line to become slack at higher angles could cause the wing to enter the lower angle-of-attack range inadvertently where luffing of the canopy could occur. It is, of course, considered imperative that flight conditions in which the canopy becomes unloaded be avoided because of the possibility that all the support cables might become slack and control of the vehicle then be lost. Although no data were obtained on the dive configuration with the model inverted, the attempts to fly

the wing in the original position with the model inverted indicated that the wing was just as unflyable in the inverted position as in the upright position. This observation should substantiate to some extent the applicability of the present test results in regard to possible unsatisfactory characteristics of the dive configuration tested.

Pitching-moment characteristics through the angle-of-attack range for the glide and dive configurations (figs. 6 and 8) indicated that longitudinal trim was not achieved for the basic boltrope condition and the moments were negative throughout the test angle-of-attack range. It is believed, however, that longitudinal trim could be obtained with a relatively small change in rigging. This failure to achieve longitudinal trim was not entirely unexpected inasmuch as a number of important factors affecting trim are difficult to control precisely in the construction of wings having flexible, cloth canopies. For example, the stiffness of the cloth at the trailing edge can have an effect on pitching moments as evidenced in unpublished data by the fact that insertion of a nylon boltrope in a slack condition gave a measurable negative pitching-moment increment from the condition of no boltrope in the trailing edge. Also, the details of cloth attachment at the leading edges and keel and of boltrope attachment at the wing tip may have an effect on the pitching moments. It is apparent from these observations and from experience with conventional airplane configurations that precise definition of longitudinal trim characteristics may not always be expected from wind-tunnel tests of small-scale models. The desired trim conditions for a flight vehicle will be affected by the boltrope length required for minimizing trailing-edge flutter and possibly the rigging would have to be altered on the basis of flight experience until the proper adjustments for a particular configuration have been defined. Another approach to the trim problem and the very low stability at low angles of attack mentioned previously might be to alter the basic rigging or attachment points so that the proper conditions could be attained in flight and this could be achieved on the present model configuration by providing an appreciable positive increment of pitching moment for a given configuration.

Effect of Keel Attachment Location

A possible means for obtaining a positive pitching-moment increment would be to move the keel attachment points rearward, and some test results showing effects of this type of modification are presented in figure 13. These results indicate some minor differences in lift curves and essentially no effect on drag coefficients or lift-drag ratios at a given lift coefficient for the basic and modified attachment points. In the low angle-of-attack range there was a positive increment in pitching moment but the rearward attachment point was not moved sufficiently far to provide longitudinal trim for the 4-percent boltrope condition. A somewhat greater movement of the attachment points (possibly 2 or 3 inches) would be required to provide trim for the glide configuration as rigged. Movement of the attachment points had little overall effect on the cable-tension coefficients presented in figure 9; however, there was a slight shift in relative load carried in the keel lines. The diagonal line carried somewhat more tension and the front and rear lines carried less tension when the attachment was moved rearward 1 inch.

Wing-Alone Characteristics

Aerodynamic characteristics in pitch of the wing alone over a fairly wide range of angles of attack were determined for the two boltrope conditions tested on the complete configuration and are presented in figures 14(a) and 14(b). These results were obtained with the wing keel attached to the six-component strain-gage balance that supported the spacecraft in tests of the complete configuration. The results presented in figure 14(a) were obtained with the center line of the keel parallel to the axis of the balance and support sting ($\gamma = 0^\circ$) and the maximum angle of attack attained was limited to about 40° by the travel of the sting support system. Inasmuch as the wing angle of attack for the flare configuration was in excess of 45° (fig. 7), it was desirable to extend the angle-of-attack range for the wing-alone data. Results are presented in figure 14(b) for the 4-percent boltrope condition with the wing mounted on a bracket that inclined the keel with respect to the balance center line ($\gamma = 7.67^\circ$). The moment reference point for both model orientations was located on the center line of the keel, 50 percent of the keel length aft of the apex center-line intersections.

Aerodynamic characteristics of the wing were obtained for dynamic pressures of 10 and 12 pounds per square foot and, with the exception of pitching moments, the data were in good agreement. (See fig. 14(a).) Pitching moments obtained with 4-percent boltrope were in good agreement at the two test dynamic pressures; however, the characteristics obtained with the boltrope slack showed more positive pitching-moment coefficients at the higher dynamic pressure. This effect of dynamic pressure can be interpreted as another indication of the sensitivity of the pitching moments to the trailing-edge conditions. Apparently the higher dynamic pressure caused the fabric to deform at the trailing edge with the boltrope slack in a manner not possible when the trailing edge was restrained by the 4-percent boltrope condition. It is interesting to observe that the effects of dynamic pressure with the boltrope slack were quite small on the other measured components and had only a relatively small effect on x_{cp} (less than 1 percent l_k). The data obtained with $\gamma = 7.67^\circ$ (fig. 14(b)) were not quite as smooth as the previously discussed results; however, the overall agreement between the two sets of data was good.

Spacecraft Alone

Aerodynamic characteristics in pitch of the spacecraft are presented in figure 15 for the purpose of obtaining a direct indication of the contribution of the spacecraft aerodynamic characteristics to the complete configuration. These results show that throughout most of the angle-of-attack range the spacecraft lift coefficient was about 0.01 and the drag-coefficient contribution was about 0.035.

Comparison of Characteristics Obtained From Balance Data and Cable-Loads Data

Very little work has been done prior to the present study on determination of cable loads and aerodynamic characteristics of cable-connected configurations,

and further assessment of the experimental techniques used in obtaining the present data was considered desirable. All the cable and wing angles of attack presented herein were obtained from photographs of the model at each test point, and obtaining the angles involved corrections to the measured angles in order to go from the plane of the camera to the desired plane on the model. In order to obtain an indication of the overall accuracy in measurement and correction of cable angles and to determine the consistency of the line-loads data and the overall characteristics, the line-loads data have been summed and compared with balance data. The cable angles presented in the data of figures 6 and 7 were used to resolve the tension coefficients into lift and drag components with respect to the capsule for comparison with the data for the complete configuration. These comparisons are presented in figures 16 and 17 for the glide and flare configurations. Pitching-moment characteristics were obtained from the cable-tension data by summing the pitch contribution of each cable at the attachment points. A similar summation was made to compare with the wing-alone data in which the reactions at the wing attachment points were used and the moments were determined about the moment reference for the wing alone. This comparison is presented in figure 18.

The comparison of data for each of the complete configurations (figs. 16 and 17) shows very good agreement in the trends with lift coefficient for all the measured components. Significant differences in drag coefficient at a given lift coefficient are indicated for each configuration; however, this difference is to be expected inasmuch as the cable loads did not include the drag of the spacecraft. It is interesting to note that although there were some differences in pitching moments at a given angle of attack or lift coefficient, the break in the pitching-moment curve at low angles of attack was in good agreement for the two sets of data.

The agreement between cable-loads data and six-component-balance data for the wing alone was very good as regards the variation with lift coefficient. The higher drag obtained from the cable-loads data cannot in this instance be attributed to spacecraft drag and reasons for this discrepancy are not known. The dotted-line curves shown in figure 18 for the wing-alone balance data were obtained from the data with $\gamma = 0^\circ$ and $\gamma = 7.67^\circ$ and represent a faired variation of characteristics from the two sets of data.

Considerations of Test Technique and Model Simulation

The present investigation of cable-supported configurations required a different method of testing from those previously used, and it is desirable to examine the possible limitations of the model simulation and experimental techniques used. Some of the factors that could have an effect on the applicability of the present results are considered briefly.

Mass and elastic characteristics of the model.- It would, of course, be desirable to duplicate exactly, for a model wing, the mass characteristics of the full-scale wing for which the data are to be obtained. This proper simulation, however, may not be feasible in some instances inasmuch as scaling of the wing fabric can be difficult and proper scaling of the elasticity, inertias, and weight

of the wing and attachments may not be practical. Inasmuch as these characteristics were not available for simulation by the present model, the wing structure was made as simple and lightweight as feasible. The experimental approach taken in the present study was to obtain data throughout a range of dynamic pressure for each design rigging with the model upright and inverted to determine the dynamic pressures for which the aerodynamic effects were large enough to minimize wing weight effects. Satisfactory test dynamic pressures for the present rigid-tube model having the sweep fixed were then assumed to be defined by the relative invariance of measured data with dynamic pressure. The test results presented in figures 4 and 5 indicated that a test dynamic pressure of $q = 10$ or greater would be required to minimize wing weight effects on the measured aerodynamic characteristics and cable-tension coefficients.

The present model was intended to represent a parawing having an inflated-tube structure and the question arises as to how well the rigid model simulated an inflated-tube configuration. The data obtained at dynamic pressures above 10 pounds per square foot for each design condition with the model upright should be directly applicable to a parawing configuration having rigid leading edges and keel or for an inflated-tube configuration having a high inflation pressure sufficient to prevent appreciable bending of the keel and sweep variation along the leading edges.

An infinite mass simulation of the spacecraft was inherent in the present test technique in which the spacecraft was attached to the sting support and the wing was in flight, restrained only by the five cables connecting the wing to the spacecraft. Effects on the data of this simulation have not been evaluated; however, it is believed that these effects would not be appreciable for steady flight near the design trim conditions.

Effects of model orientation.- Test results were obtained with the model upright and inverted in order to determine if the aerodynamic forces were large enough in relation to the wing weight effects so that model orientation would not affect the results. The data of figures 9 and 10 show marked differences in lift and pitching moment with the model upright and inverted. Some differences would be expected inasmuch as the direct wing weight contribution was not included in the measured aerodynamic characteristics for the model in the inverted condition whereas for the upright condition, the measured lift, for example, was less than the aerodynamic lift by the amount of the wing weight. The magnitude of the differences shown in figures 9 and 10, however, is considerably larger than that expected from the direct weight contribution indicated in figure 19. There are also appreciable differences in cable-tension coefficients with the model upright and inverted, particularly for the diagonal line. (See figs. 9 to 12.) Measured values of wing angle of attack indicate that the wing was at an angle about 1° higher for the inverted position than for the upright position. The difference in wing angle of attack would also be expected to cause differences in measured characteristics as indicated; however, reasons for the difference in wing angle of attack are not known.

The aerodynamic characteristics of a configuration should not be a function of the test orientation of the model and the question with regard to the present results is which model orientation would be expected to yield results that would be most applicable. It would appear that the upright orientation should be

preferred because this duplicates the orientation of the flight vehicle and the main source of possible error inherent in this technique would be in possible differences in wing weight and inertia between the model and full-scale wing. The test results previously discussed indicated that the higher dynamic pressures ($q = 10$ to $q = 14$) minimized the wing weight effects for the model upright. In view of this and of the more erratic nature of the data obtained with the model inverted, it is believed that data obtained with the upright orientation of the model would be more applicable for design use.

Effects of angle of attack with a fixed rigging.- The test data obtained over a range of angles of attack appreciably above and below the design trim conditions do not apply strictly for steady-flight conditions inasmuch as with longitudinal control by center-of-gravity shift the rigging would have to be changed in order to trim at each angle of attack. It is believed, however, that the results obtained are valid for at least a limited angle-of-attack range either side of the design point for the determination of cable loads, longitudinal stability, lift, and drag. Furthermore, the present results may be considered indicative of the characteristics for a limited range of normal acceleration resulting from angle-of-attack excursions due to gusts or other disturbances in which the rigging is not changed during the excursion.

SUMMARY OF RESULTS

The results obtained in an investigation of aerodynamic characteristics and cable tension for a cable-connected parawing and spacecraft may be summarized as follows:

1. The value of maximum lift-drag ratio for the complete model was about 2.7, and for the wing alone was 3.5. The relatively large diameter of the wing leading edges and keel (7 percent of the keel length) was believed to be partly responsible for these relatively low values of lift-drag ratio.

2. Longitudinal stability for the glide and flare configurations was high near the design angle of attack for each configuration; however, for angles below the design angle of attack, the model was neutrally stable or slightly unstable. This condition of approximately neutral stability combined with the fact that the pitching moments were near zero would be considered highly undesirable for a flight vehicle. These unsatisfactory stability characteristics are believed to result from the diagonal cable between the wing and spacecraft becoming slack.

3. Test results on the distribution of cable tension in the five lines connecting the wing and spacecraft, for the design conditions, indicated that approximately 25 percent of the total tension in all lines was carried in each of the two leading-edge cables. The remaining approximately 50 percent of the total cable tension was carried in the lines to the keel, with the diagonal line carrying somewhat higher tension than the front and rear lines.

4. For angles of attack considerably below the design angle, the diagonal cable was slack and the tension measured in all the lines was relatively invariant up to about 6° below the design angle. At this point the diagonal cable began to

carry load and the tension in this line increased appreciably with angle of attack and the line carried approximately 30 percent of the total cable tension at the highest test angle of attack. In like manner the tension in the front and rear lines began to decrease, and at the highest test angle they carried approximately 8 and 12 percent of the total tension, respectively.

5. The data obtained with the six-component internal balance and from the cable tension measurements were generally in good agreement when the tension measurements were resolved into lift, drag, and pitching-moment coefficients for both the complete configuration and the wing alone.

Langley Research Center,
National Aeronautics and Space Administration,
Langley Station, Hampton, Va., May 9, 1963.

REFERENCES

1. Rogallo, Francis M., Lowry, John G., Croom, Delwin R., and Taylor, Robert T.: Preliminary Investigation of a Paraglider. NASA TN D-443, 1960.

2. Taylor, Robert T.: Wind-Tunnel Investigation of Paraglider Models at Supersonic Speeds. NASA TN D-985, 1961.

3. Naeseth, Rodger L.: An Exploratory Study of a Parawing as a High-Lift Device for Aircraft. NASA TN D-629, 1960.

4. Hewes, Donald E.: Free-Flight Investigation of Radio-Controlled Models With Parawings. NASA TN D-927, 1961.

5. Johnson, Joseph L., Jr.: Low-Speed Wind-Tunnel Investigation to Determine the Flight Characteristics of a Model of a Parawing Utility Vehicle. NASA TN D-1255, 1962.

6. Polhamus, Edward C., and Naeseth, Rodger L.: Experimental and Theoretical Studies of the Effects of Camber and Twist on the Aerodynamic Characteristics of Parawings Having Nominal Aspect Ratios of 3 and 6. NASA TN D-972, 1963.

7. Fournier, Paul G., and Bell, B. Ann: Low Subsonic Pressure Distributions on Three Rigid Wings Simulating Paragliders With Varied Canopy Curvature and Leading-Edge Sweep. NASA TN D-983, 1961.

8. Fournier, Paul G., and Bell, B. Ann: Transonic Pressure Distributions on Three Rigid Wings Simulating Paragliders With Varied Canopy Curvature and Leading-Edge Sweep. NASA TN D-1009, 1962.

9. Fournier, Paul G.: Pressure Distributions on Three Rigid Wings Simulating Parawings With Varied Canopy Curvature and Leading-Edge Sweep at Mach Numbers From 2.29 to 4.65. NASA TN D-1618, 1963.

TABLE I.- CABLE LENGTHS USED IN TESTS OF THE

PARAWING AND SPACECRAFT MODEL

Configuration	Cable length, in.[a]				
	F	D (b)	B (b)	L	R
Glide	23.7	20.06	17.36	22.75	22.75
Flare	27.66	20.72	16.74	22.70	22.70
Dive	22.23	17.91	19.67	22.26	22.26

[a]Measured from attachment point on wing to attachment point on spacecraft.

[b]The relationship $l_D + l_B = 1.25 l_K$ remained constant for all the model configurations investigated when the cable length was considered the distance between the spacecraft attachment point and the intersection of the cable and the center line of the keel.

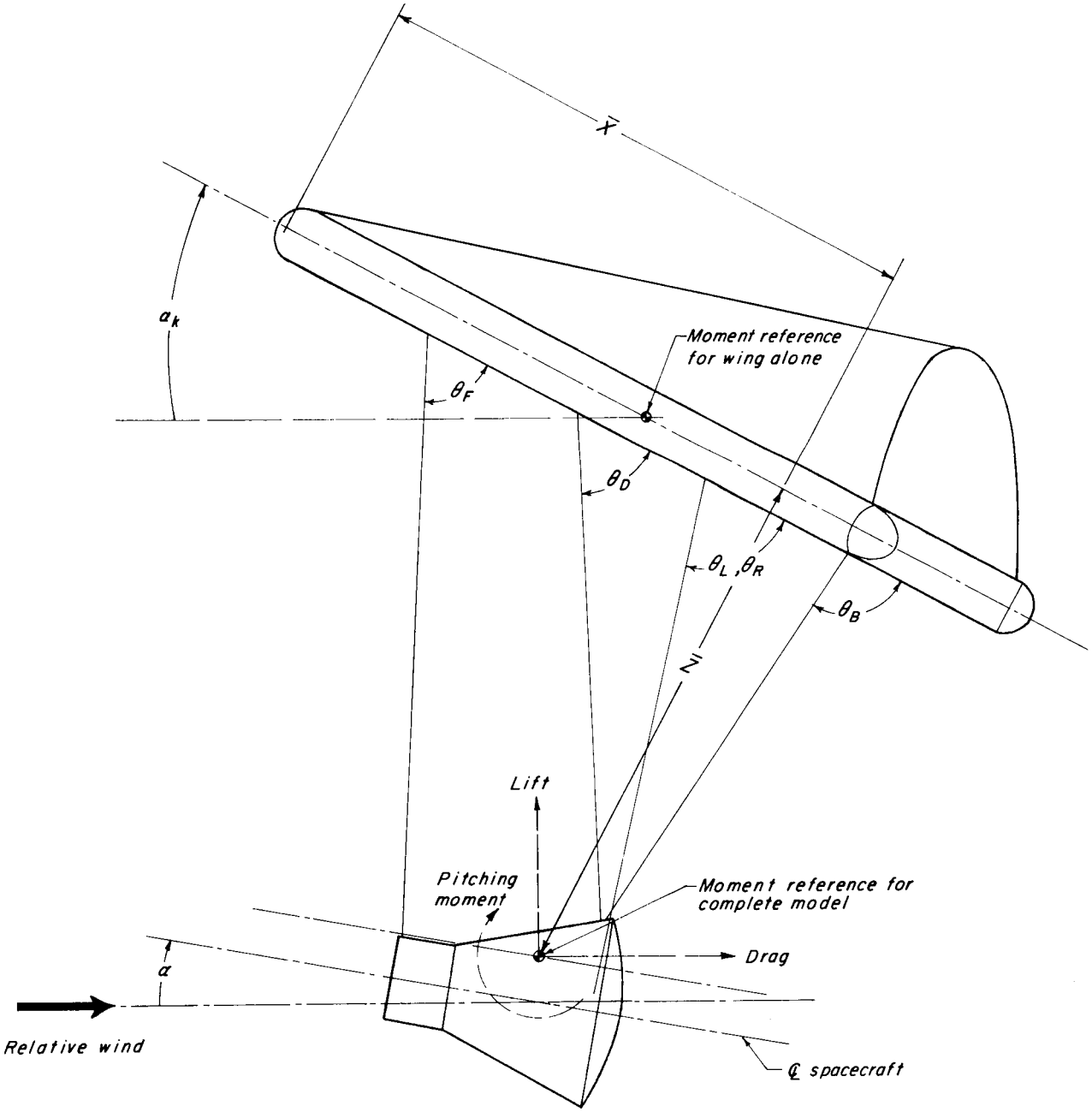

Figure 1.- System of axes used in presentation of data, showing positive direction of forces and moments.

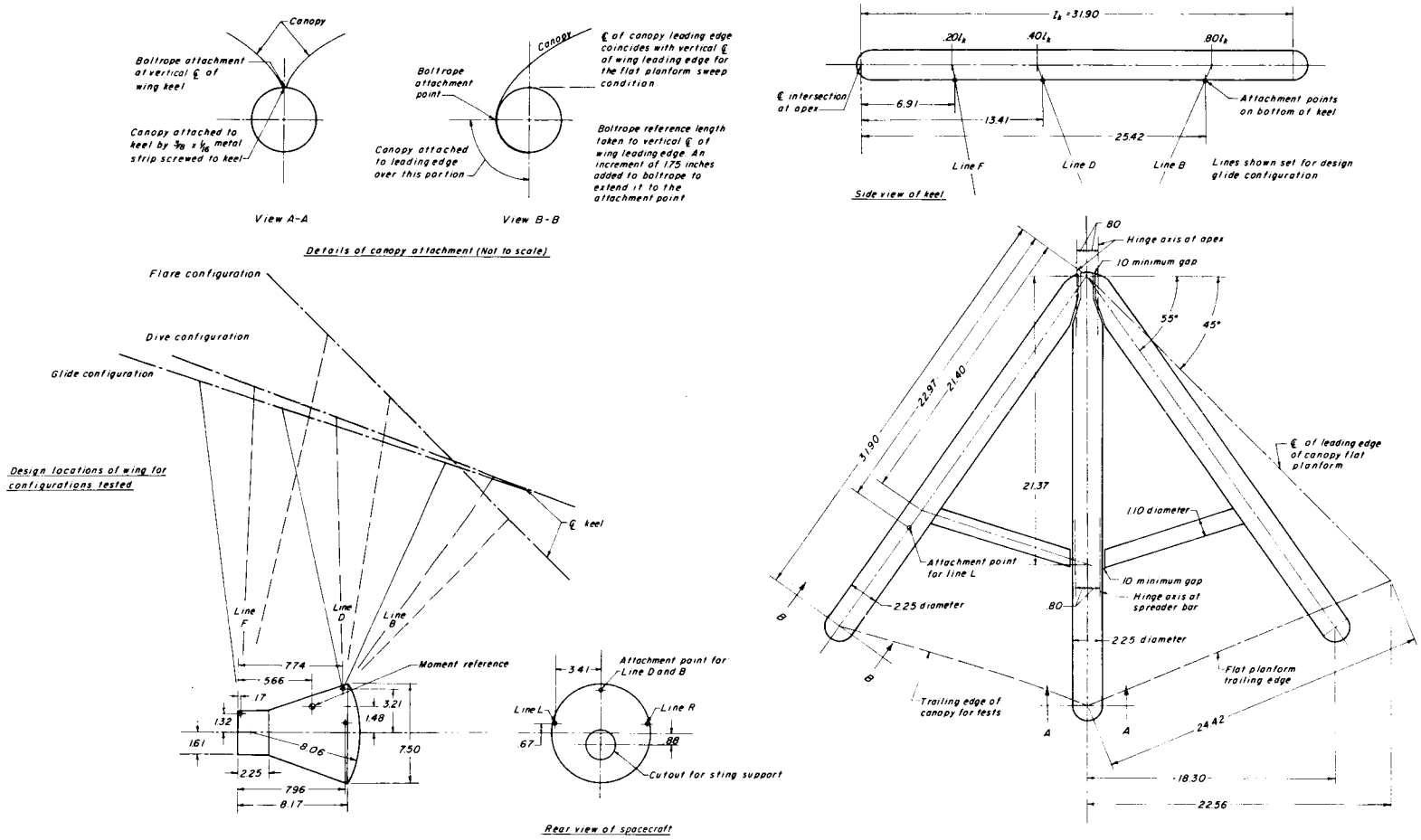

Figure 2.- General arrangement of model configuration tested. All linear dimensions are in inches.

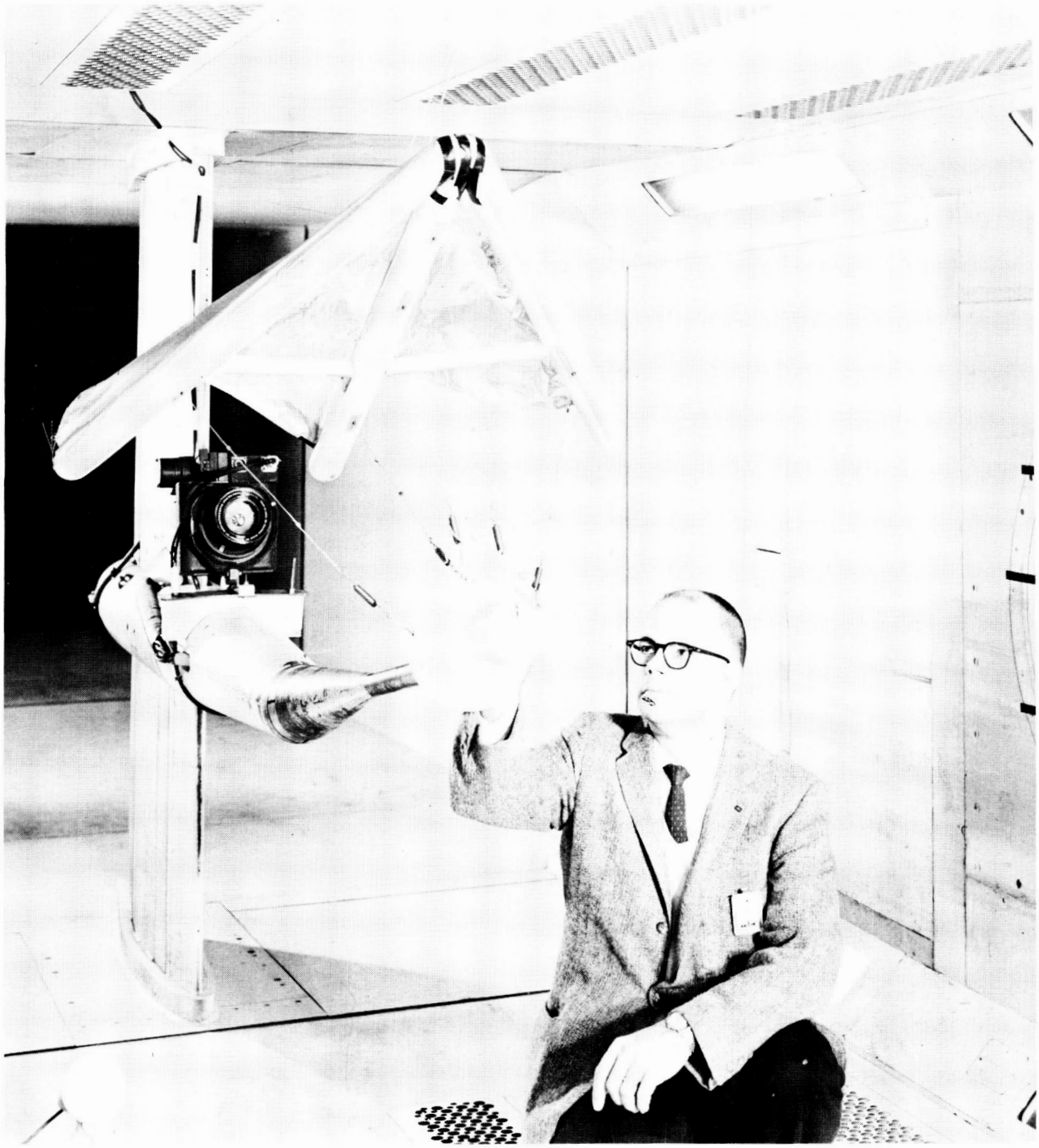

Figure 3.- Photograph of model in Langley high-speed 7- by 10-foot tunnel. L-62-816

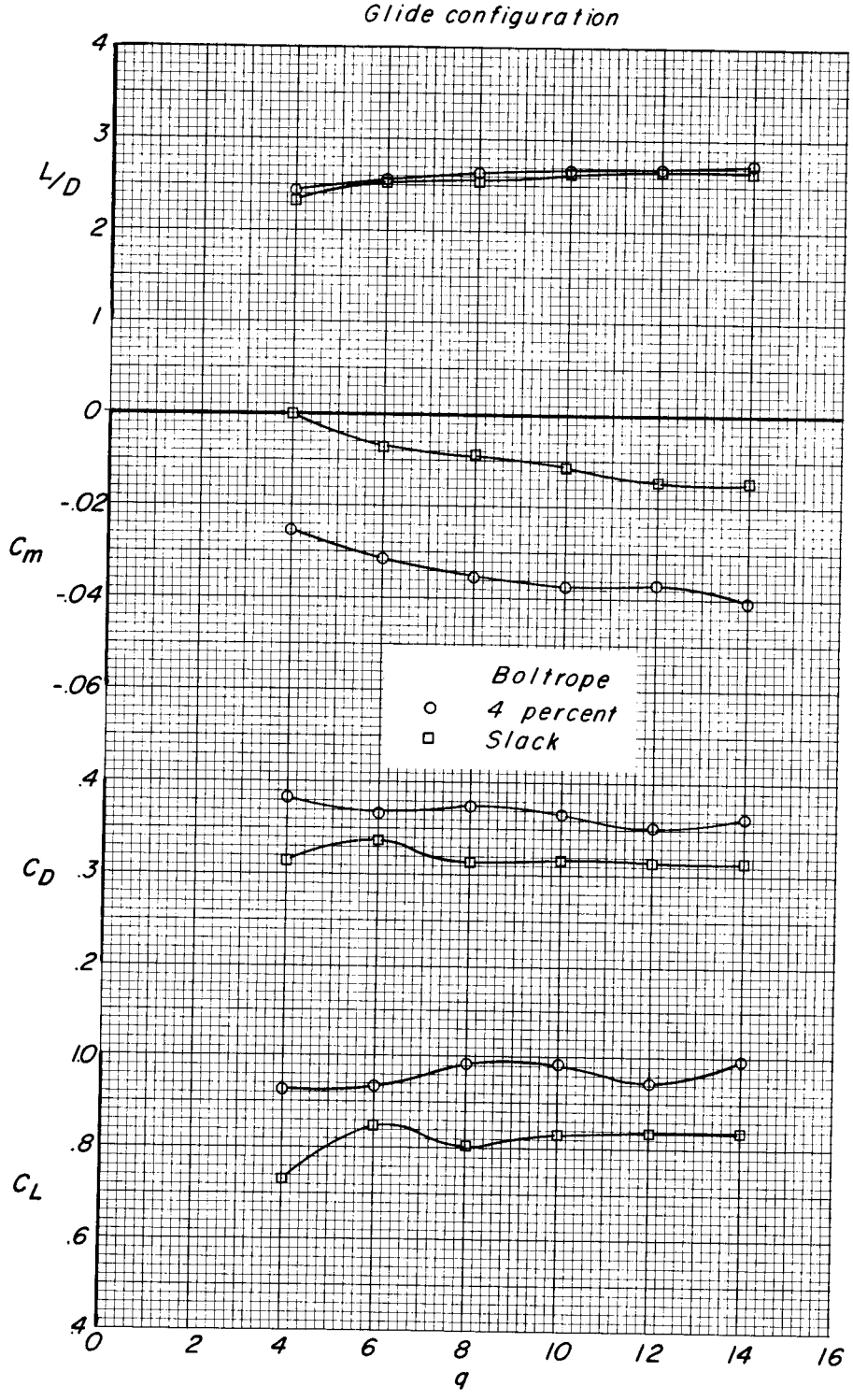

Figure 4.- Effect of dynamic pressure on aerodynamic characteristics, line loads, and wing position of glide configuration. $\alpha = 17^{\circ}$.

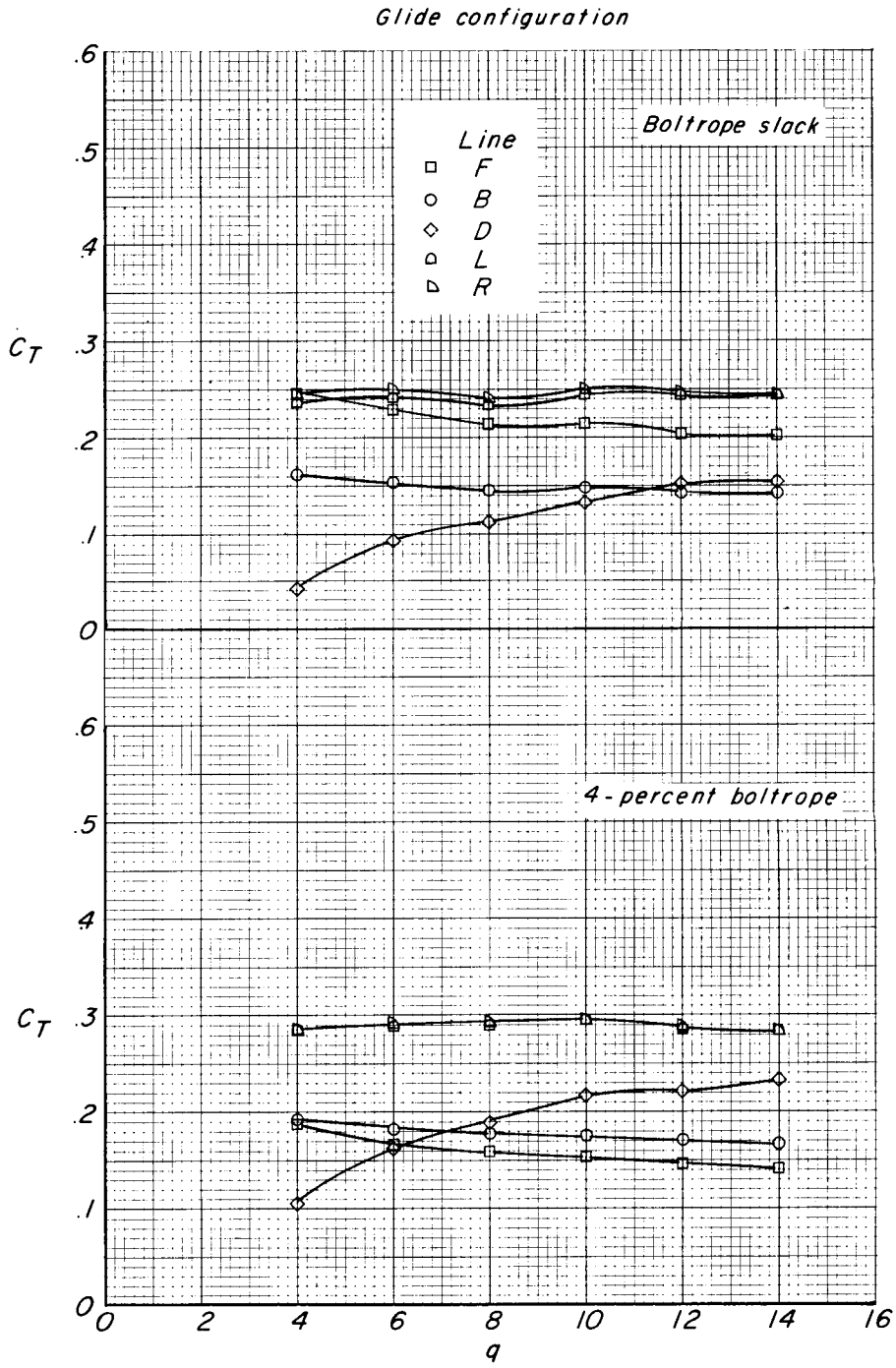

Figure 4.- Continued.

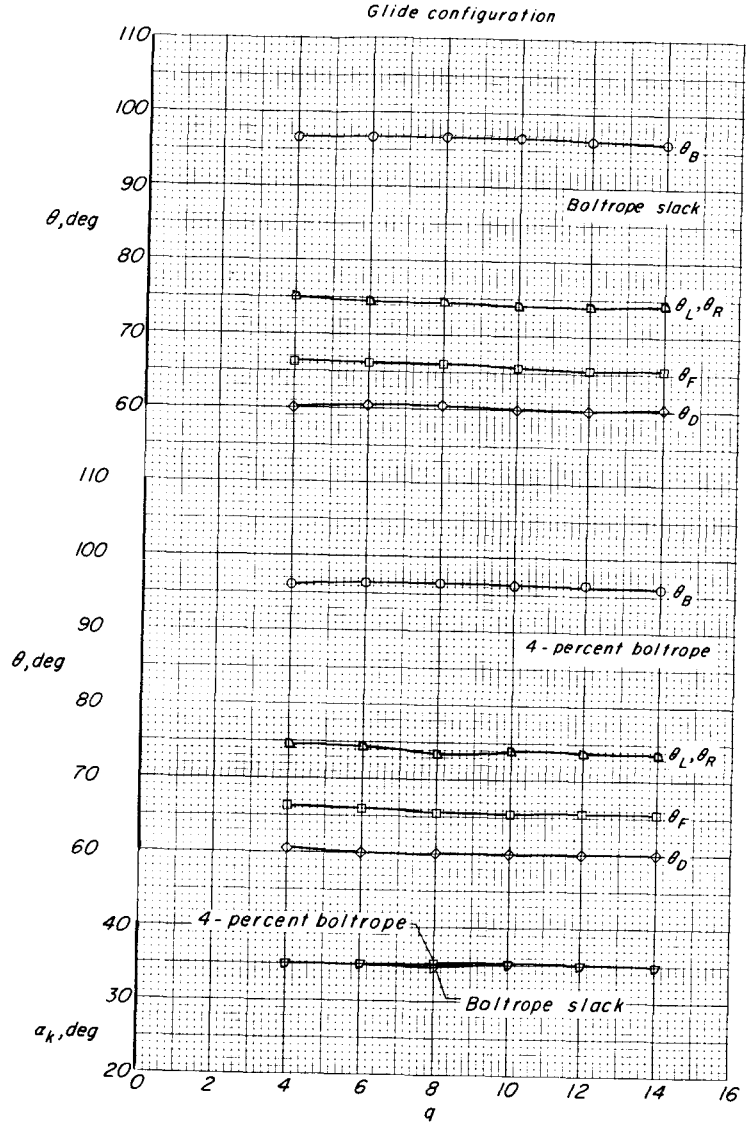

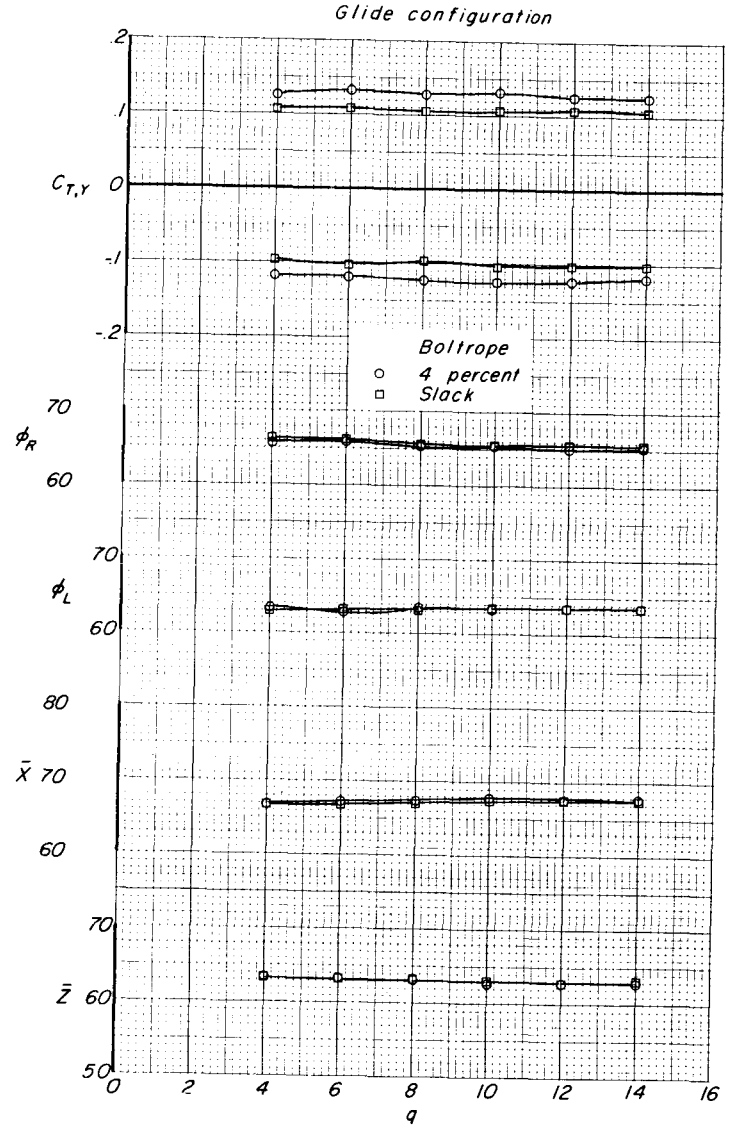

Figure 4.- Concluded.

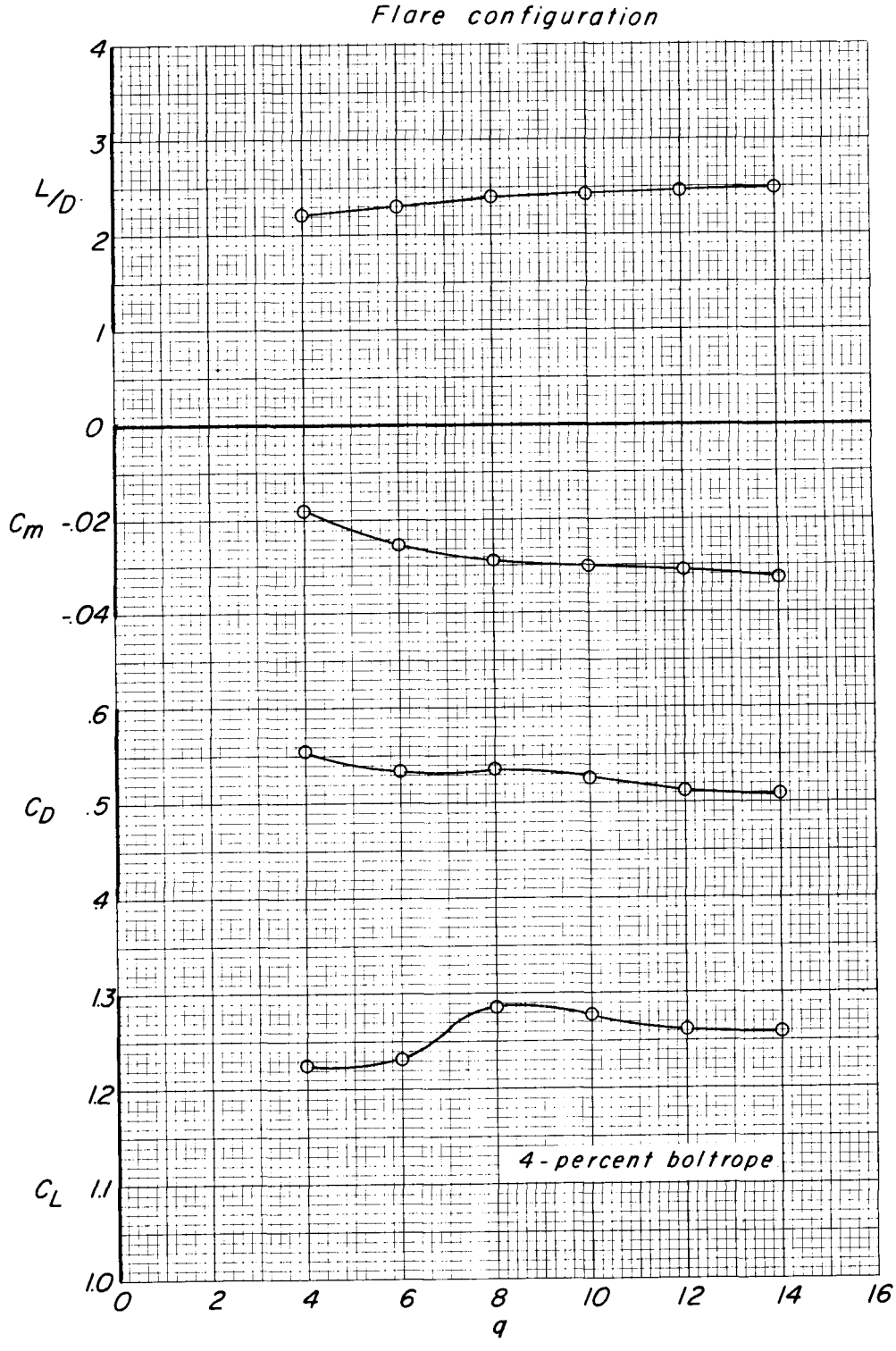

Figure 5.- Effect of dynamic pressure on aerodynamic characteristics, line loads, and wing position of flare configuration. $\alpha = 0^{\circ}$.

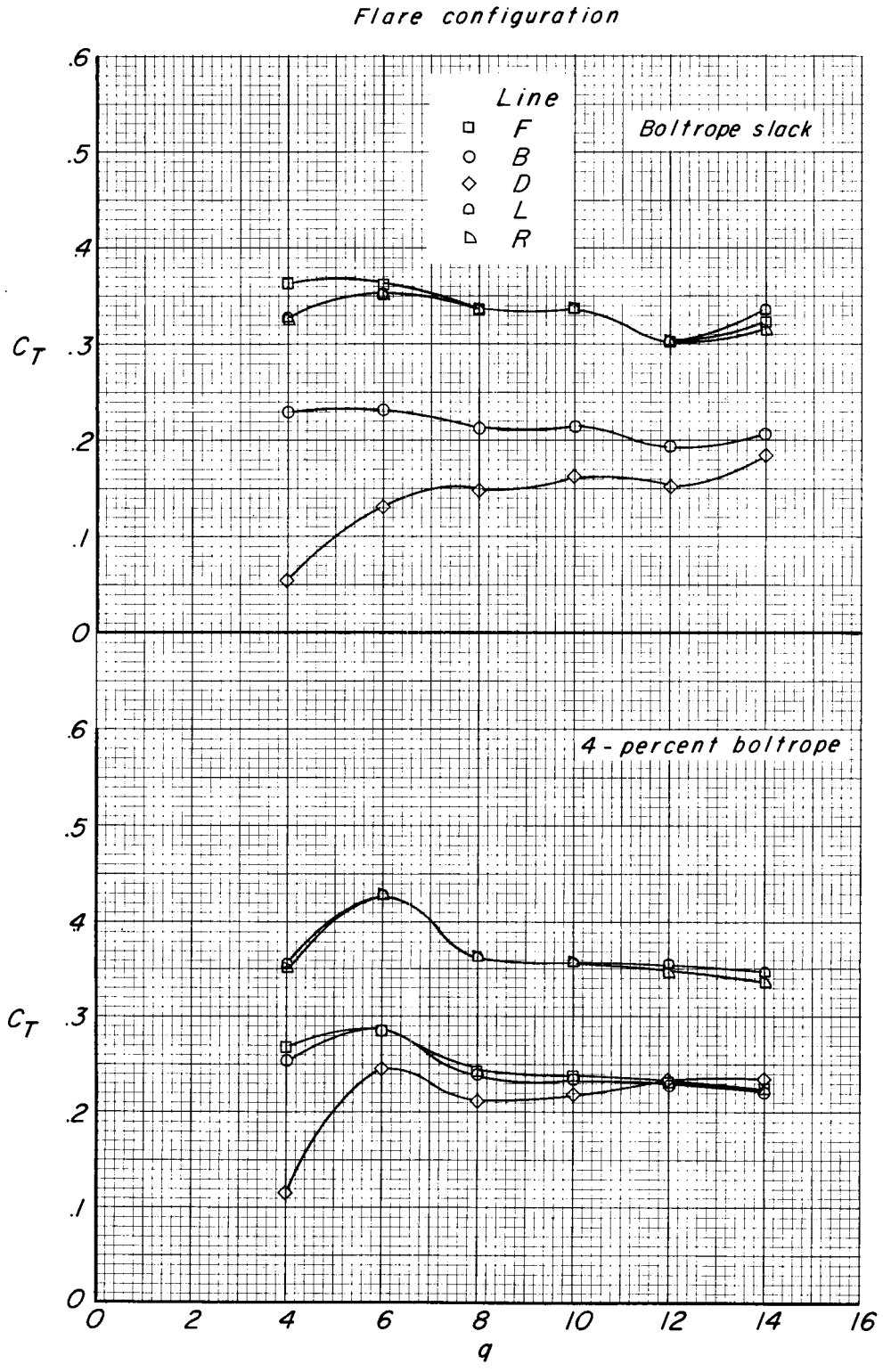

Figure 5.- Continued.

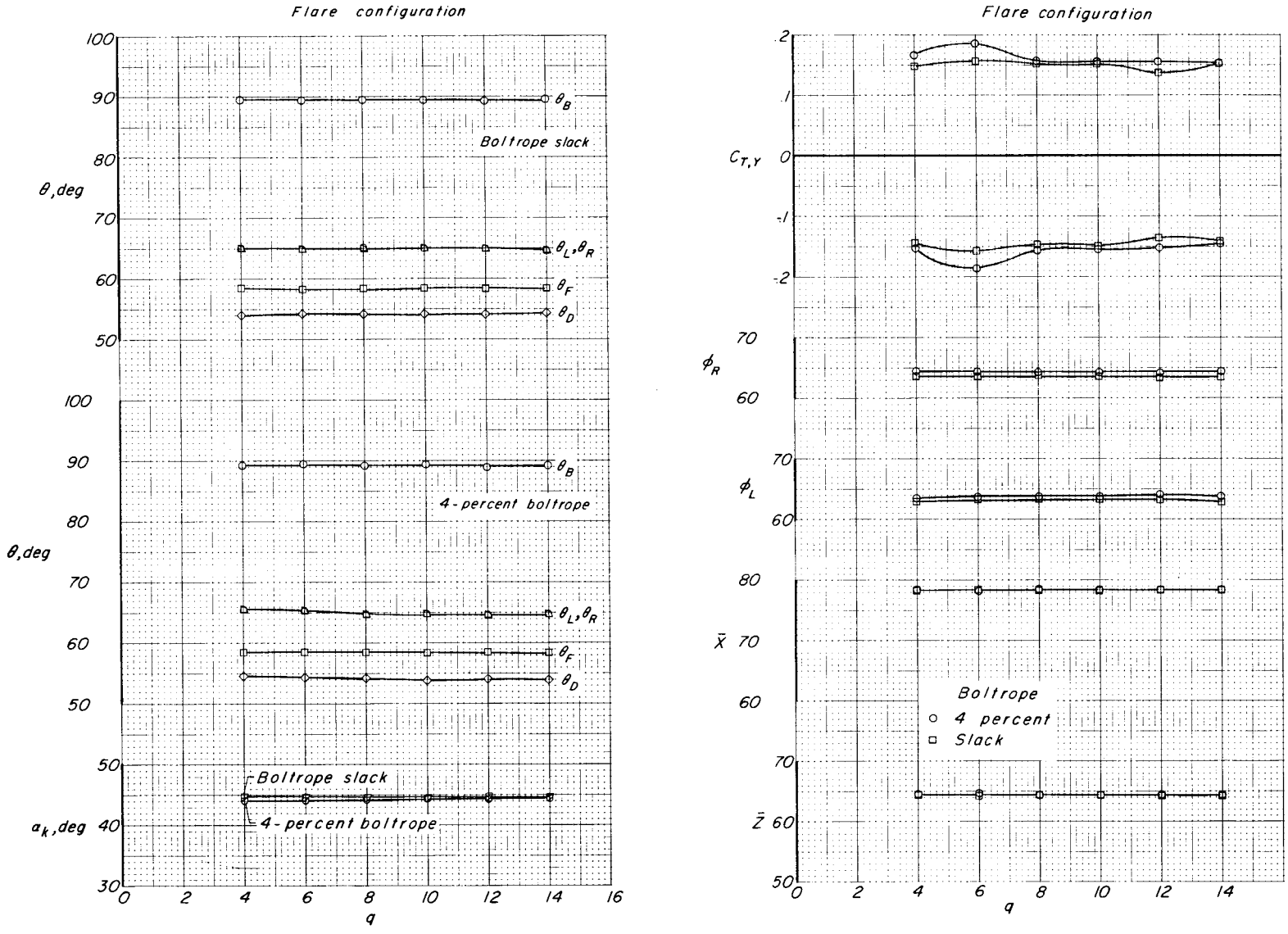

Figure 5.- Concluded.

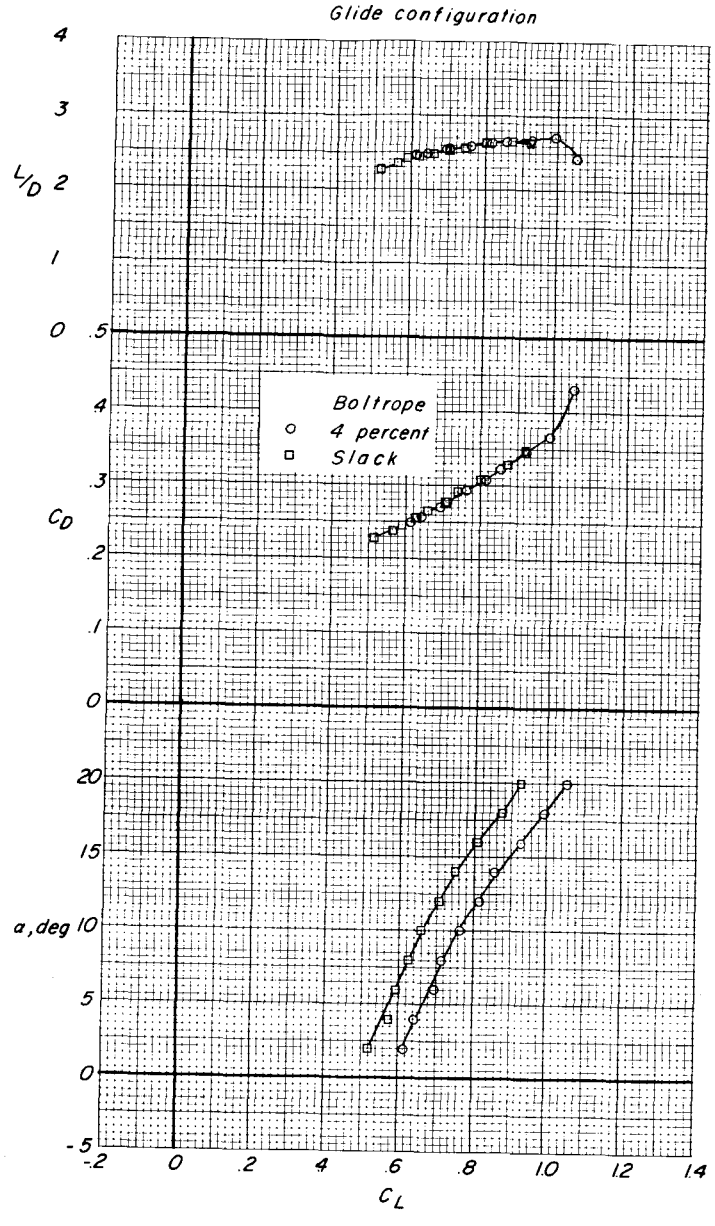

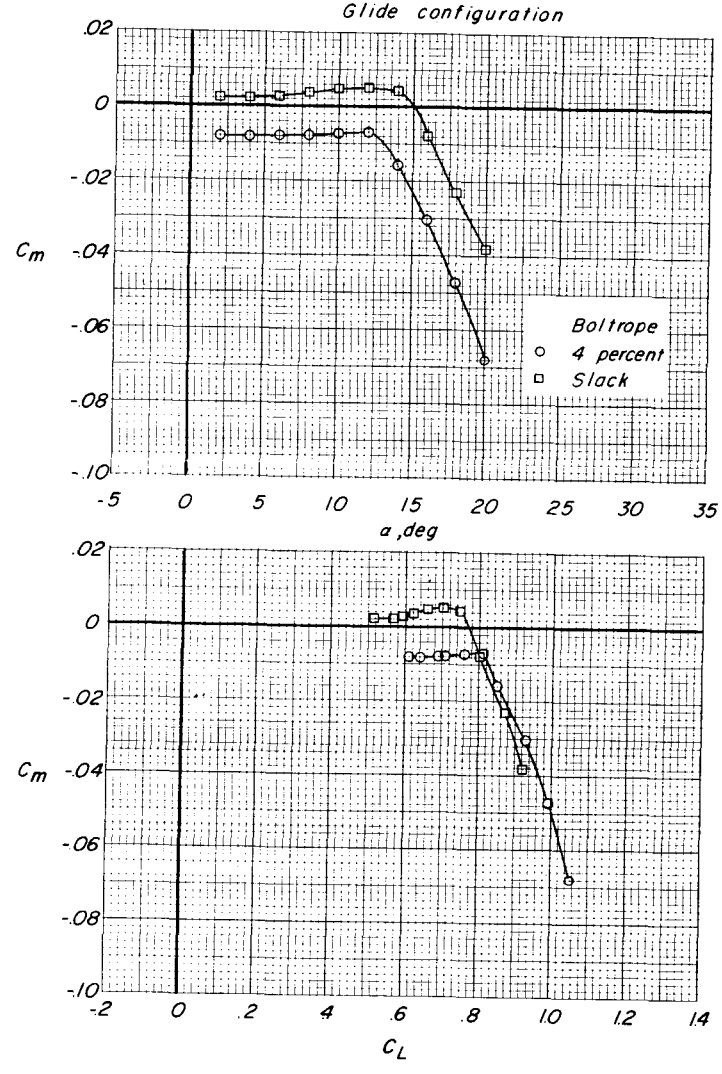

Figure 6.- Effect of angle of attack on aerodynamic characteristics, line loads, and wing position of glide configuration. q = 12.

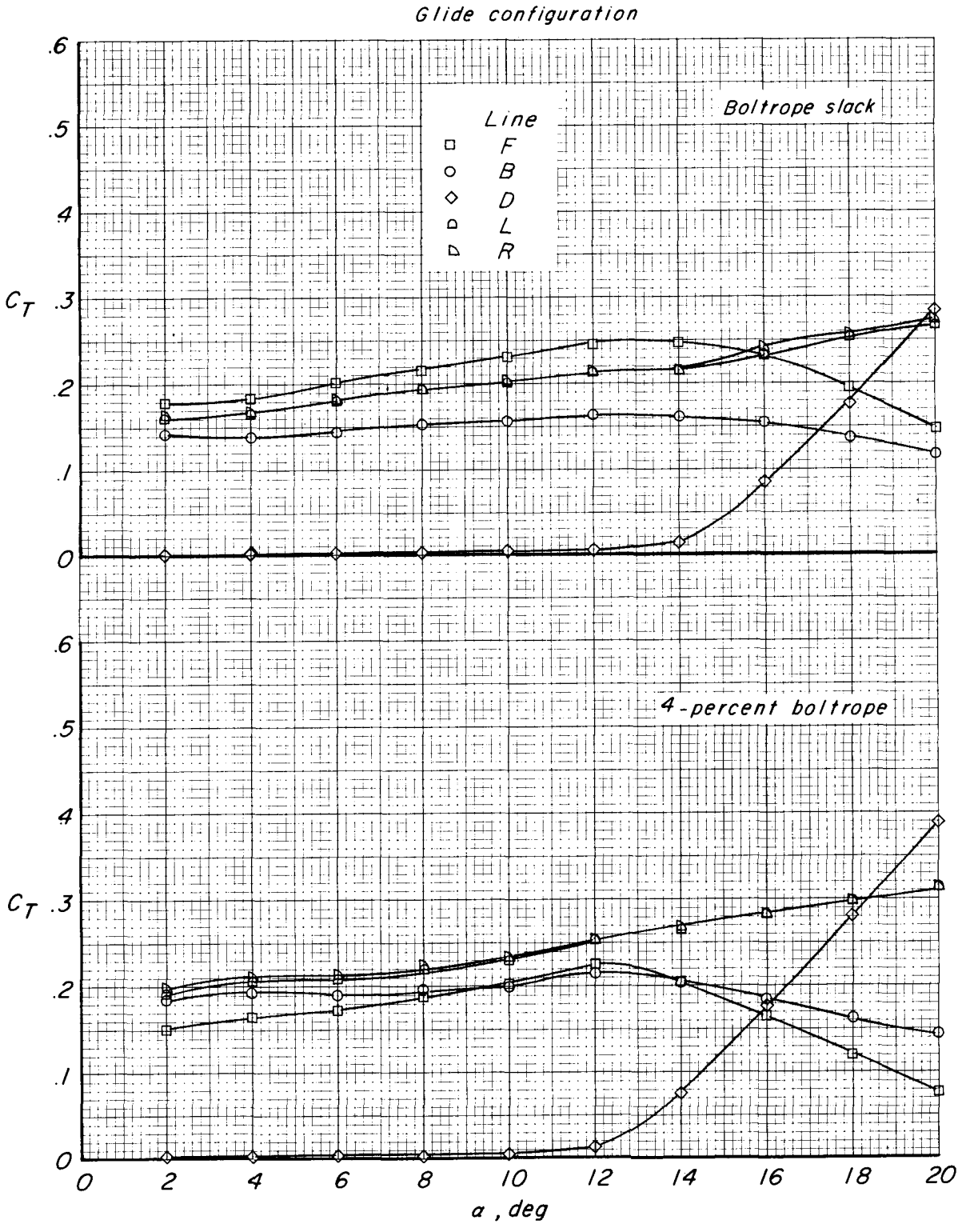

Figure 6.- Continued.

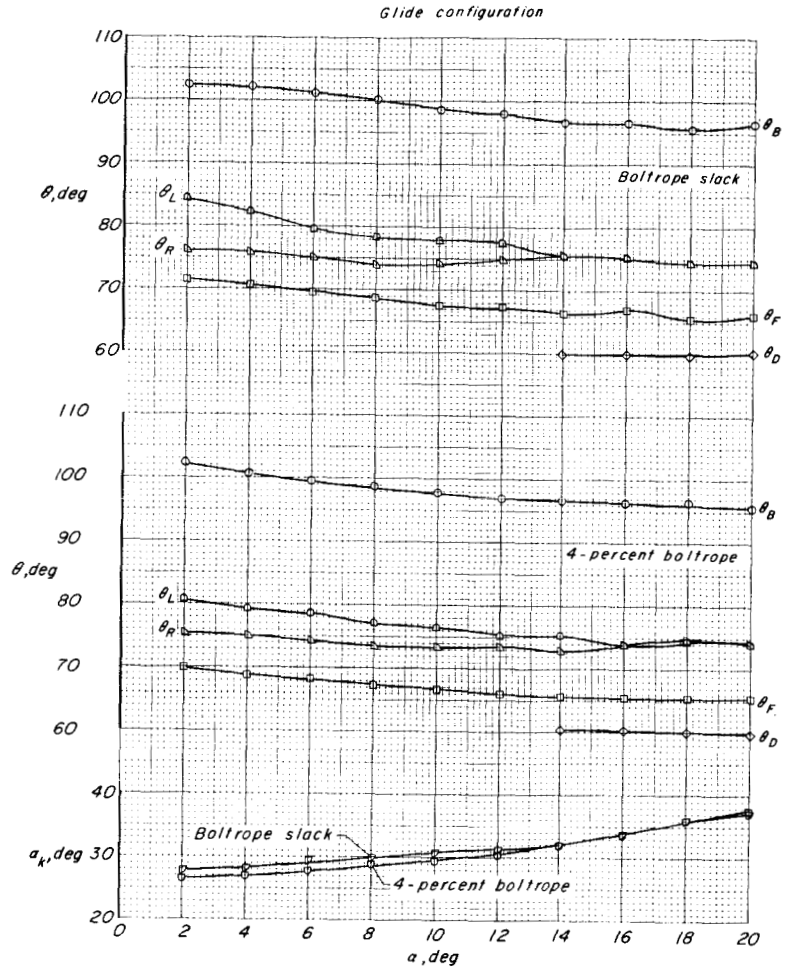

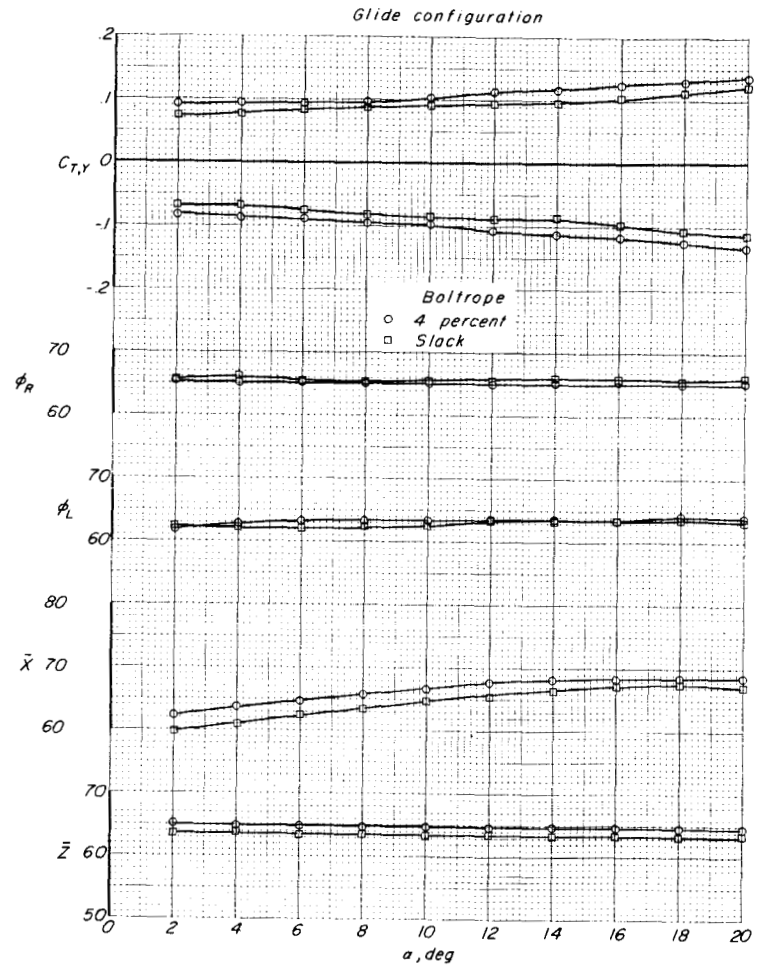

Figure 6.- Concluded.

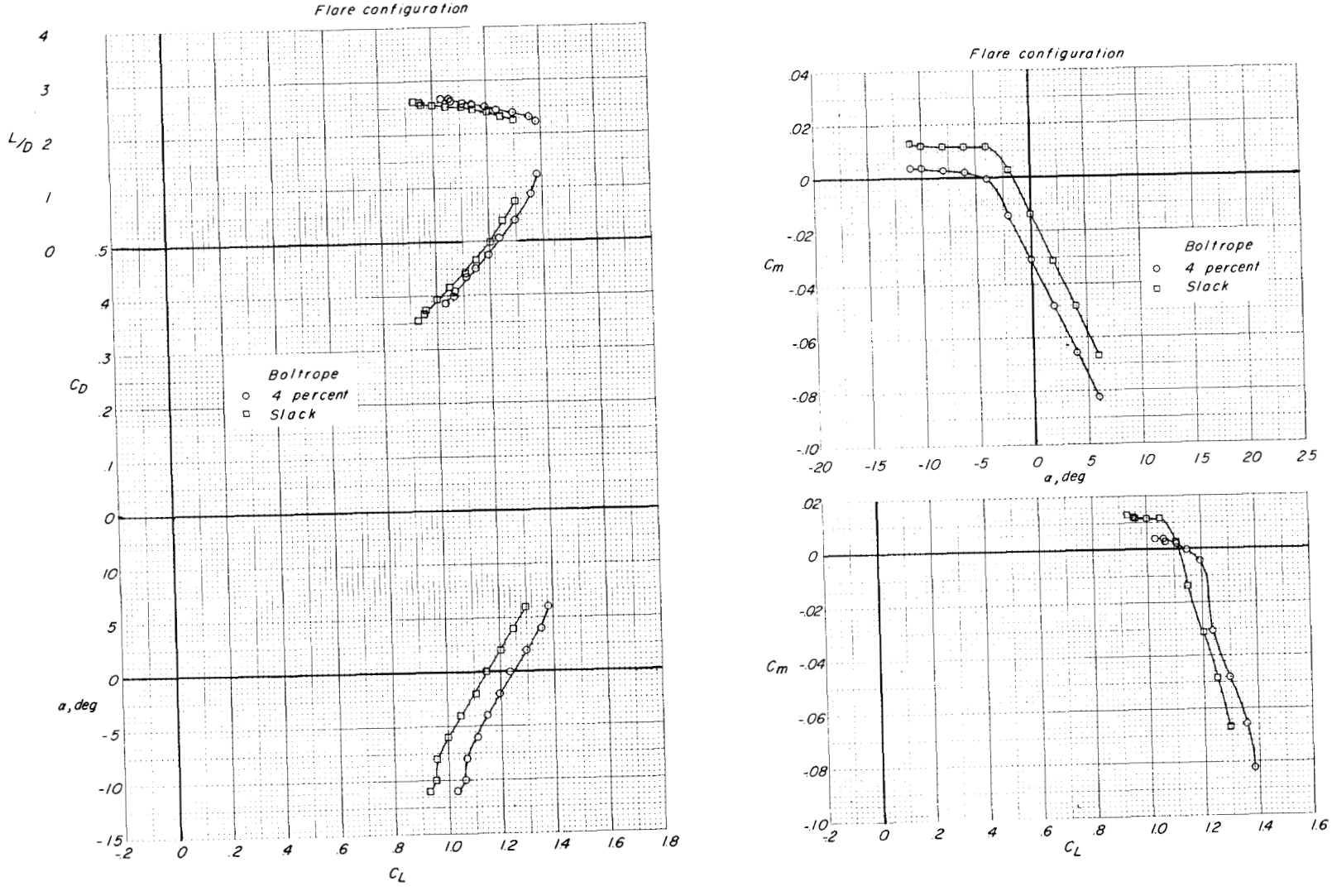

Figure 7.- Effect of angle of attack on aerodynamic characteristics, line loads, and wing position of flare configuration. q = 12.

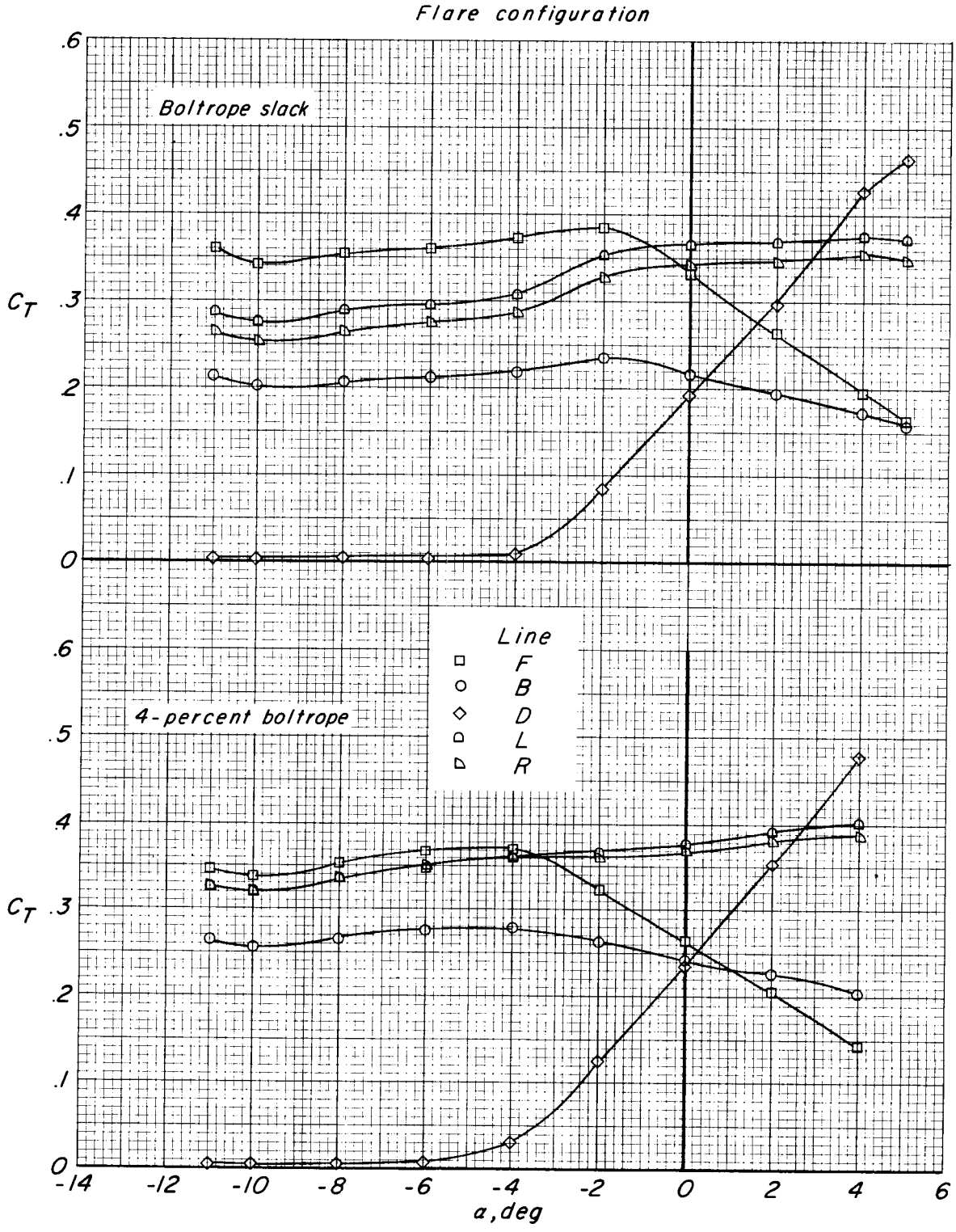

Figure 7.- Continued.

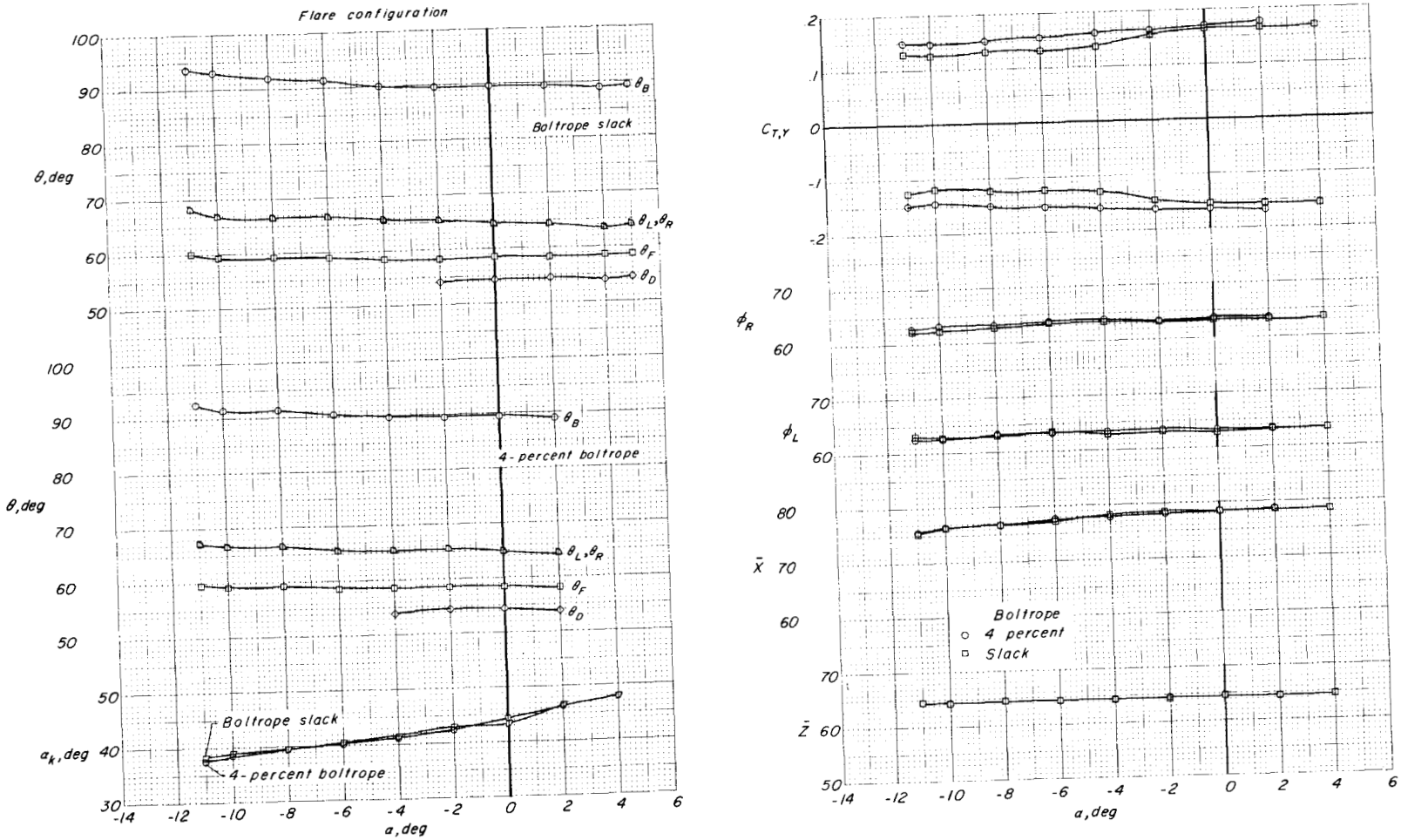

Figure 7.- Concluded.

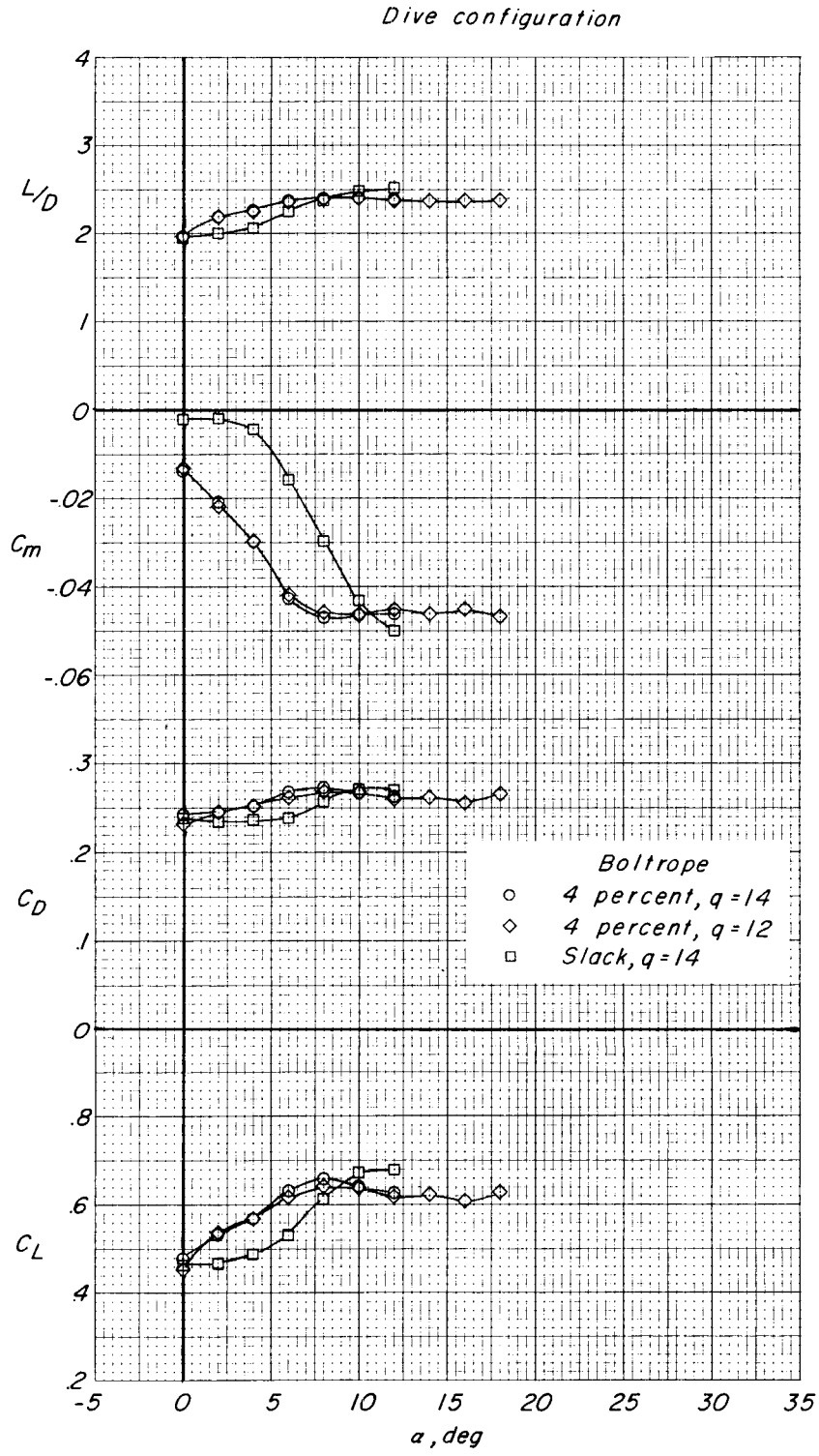

Figure 8.- Effect of angle of attack on aerodynamic characteristics, line loads, and wing position of dive configuration. q = 14.

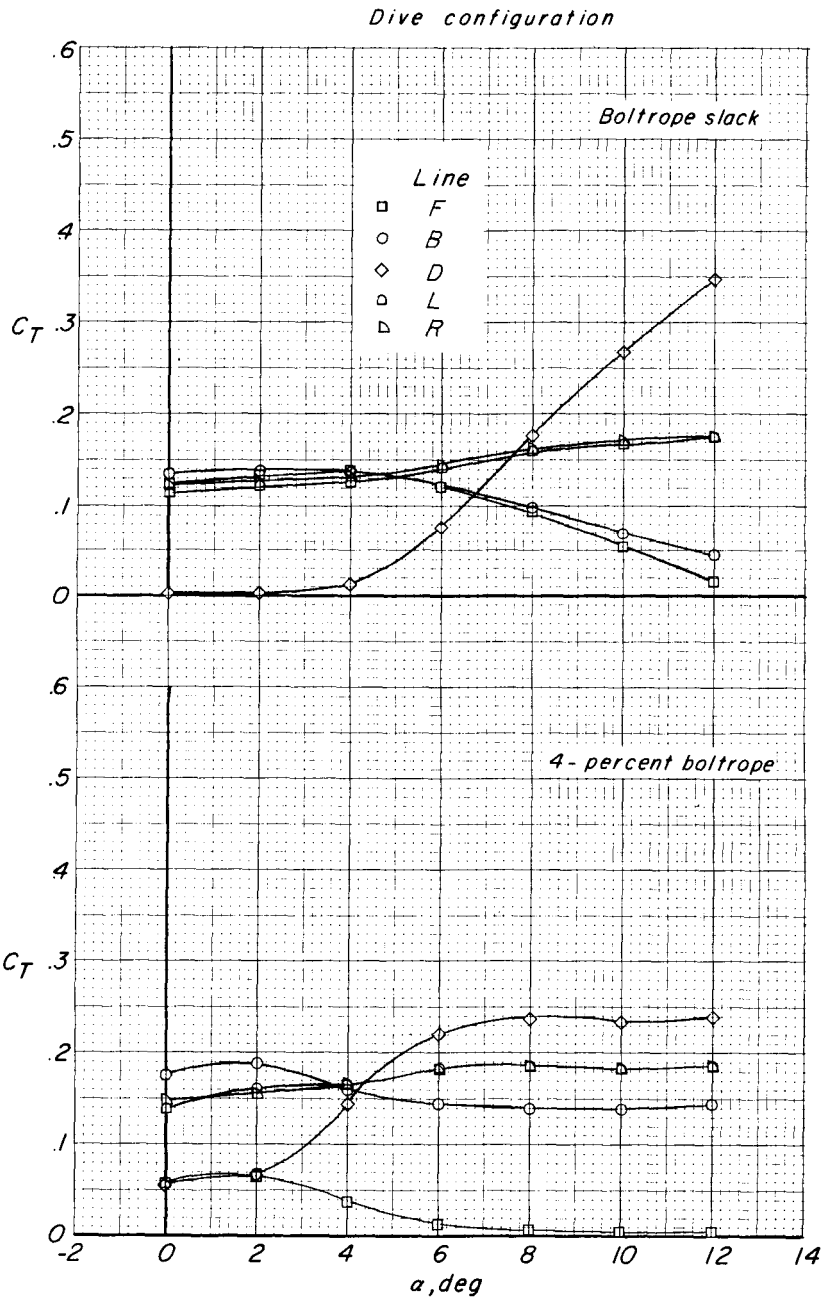

Figure 8.- Continued.

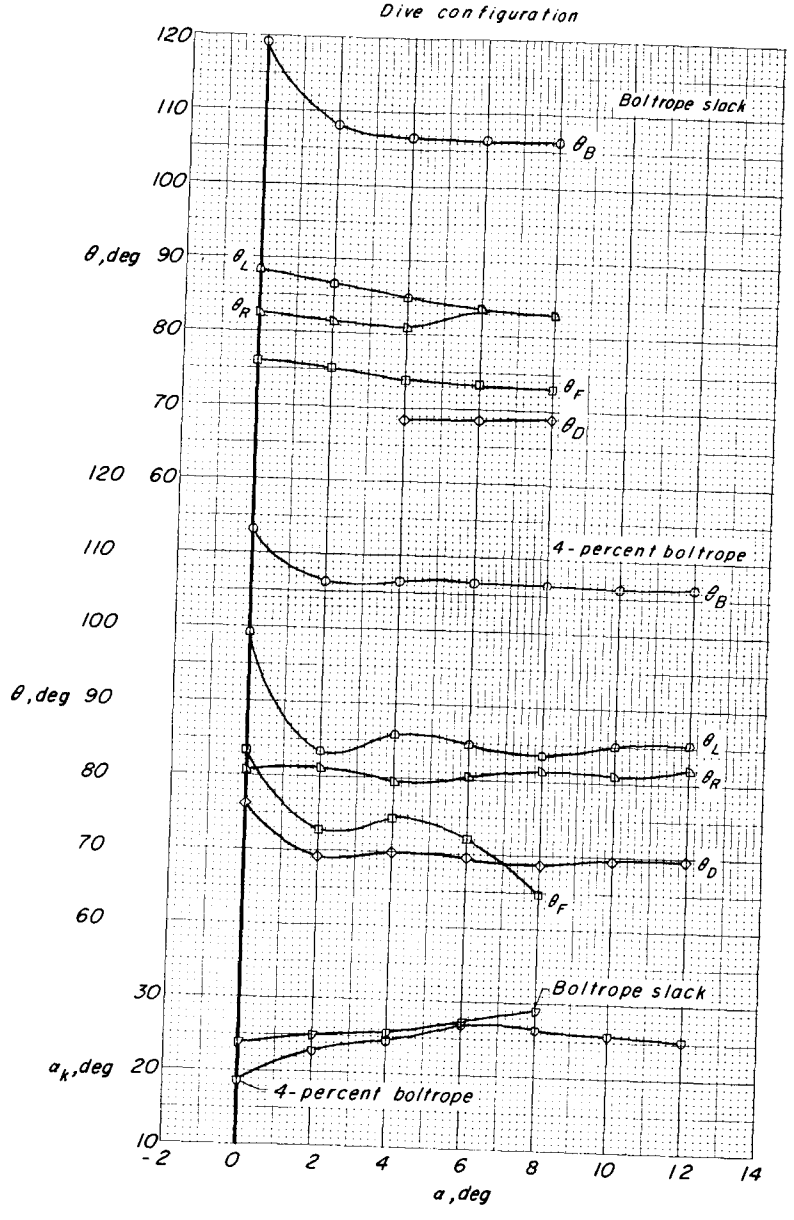

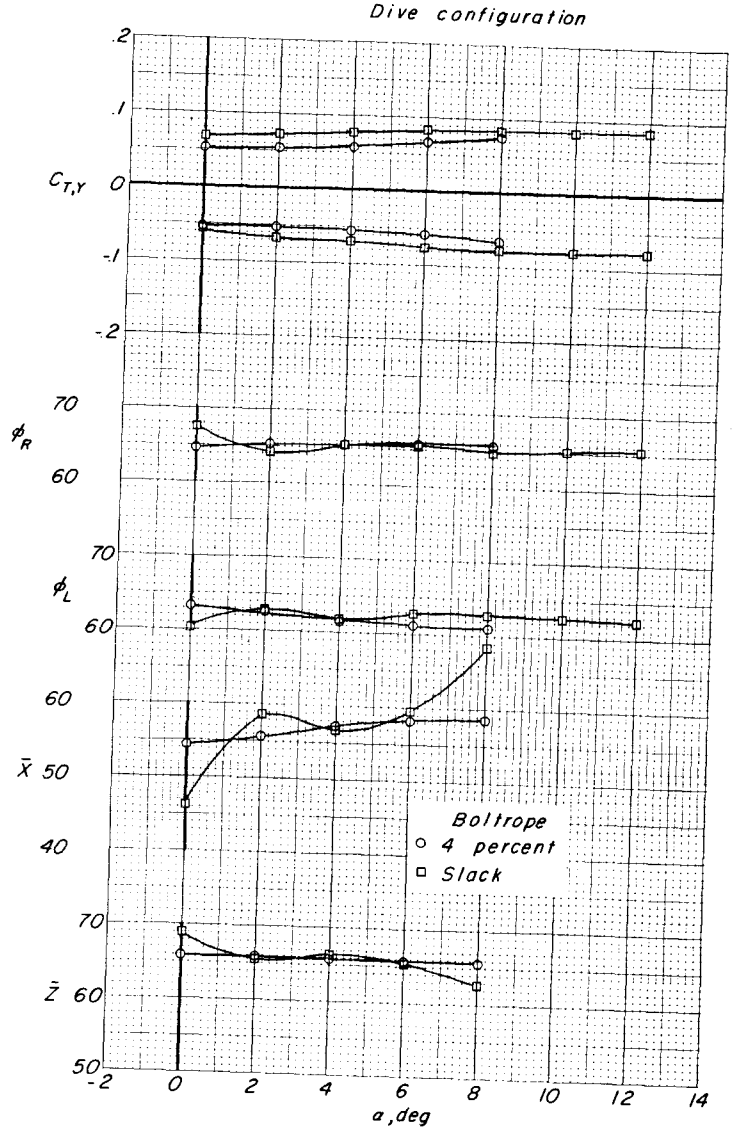

Figure 8.- Concluded.

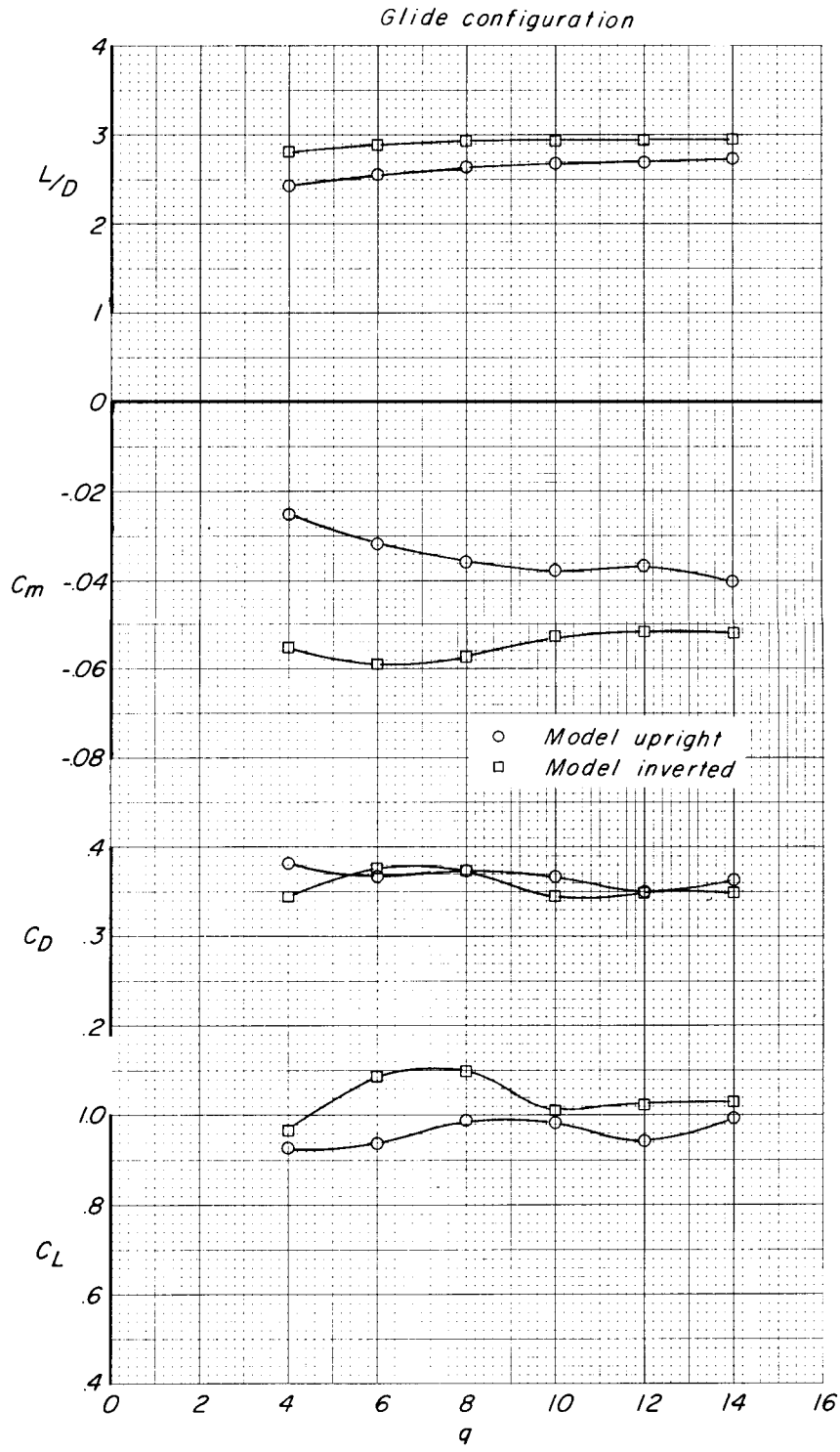

Figure 9.- Comparison of results obtained over a range of dynamic pressure with model upright and inverted for glide configuration. $\alpha = 17^{\circ}$; 4-percent boltrope.

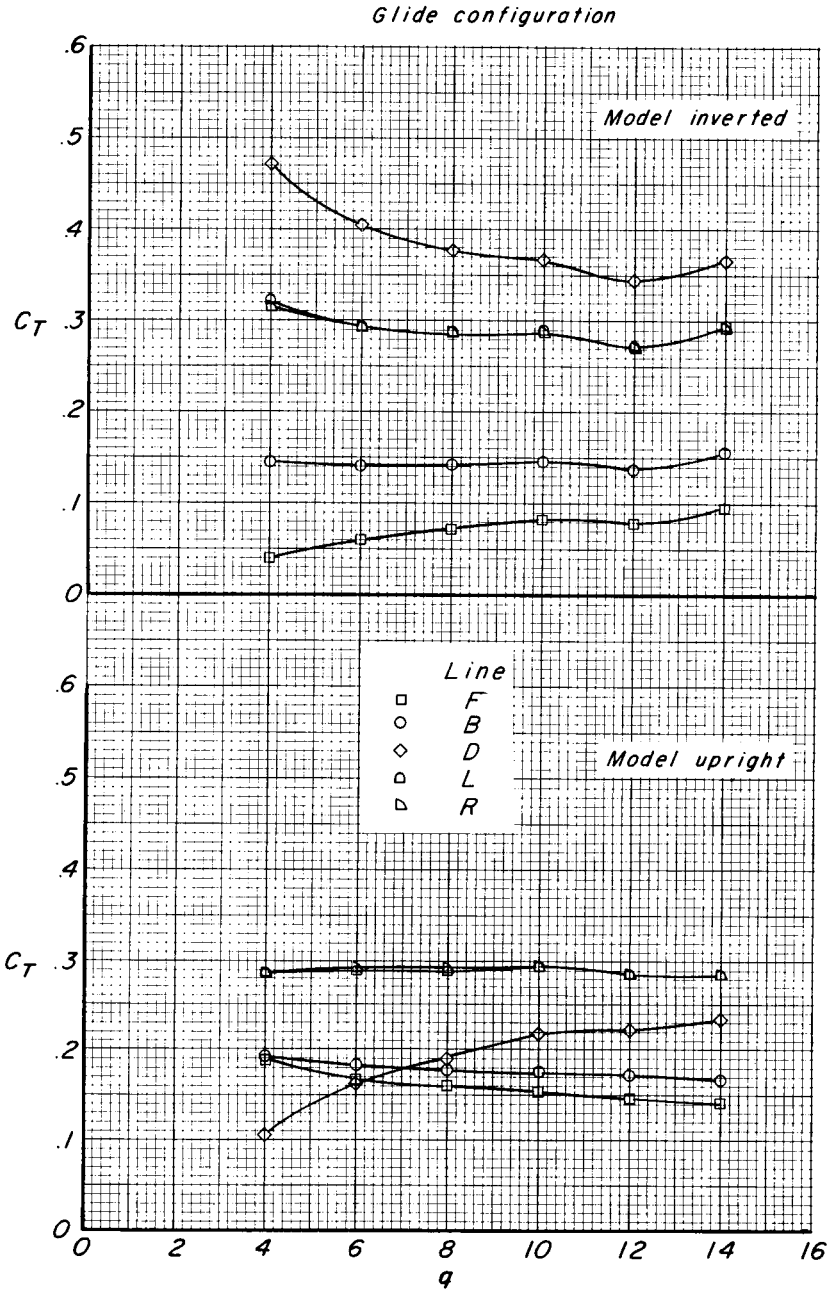

Figure 9.- Continued.

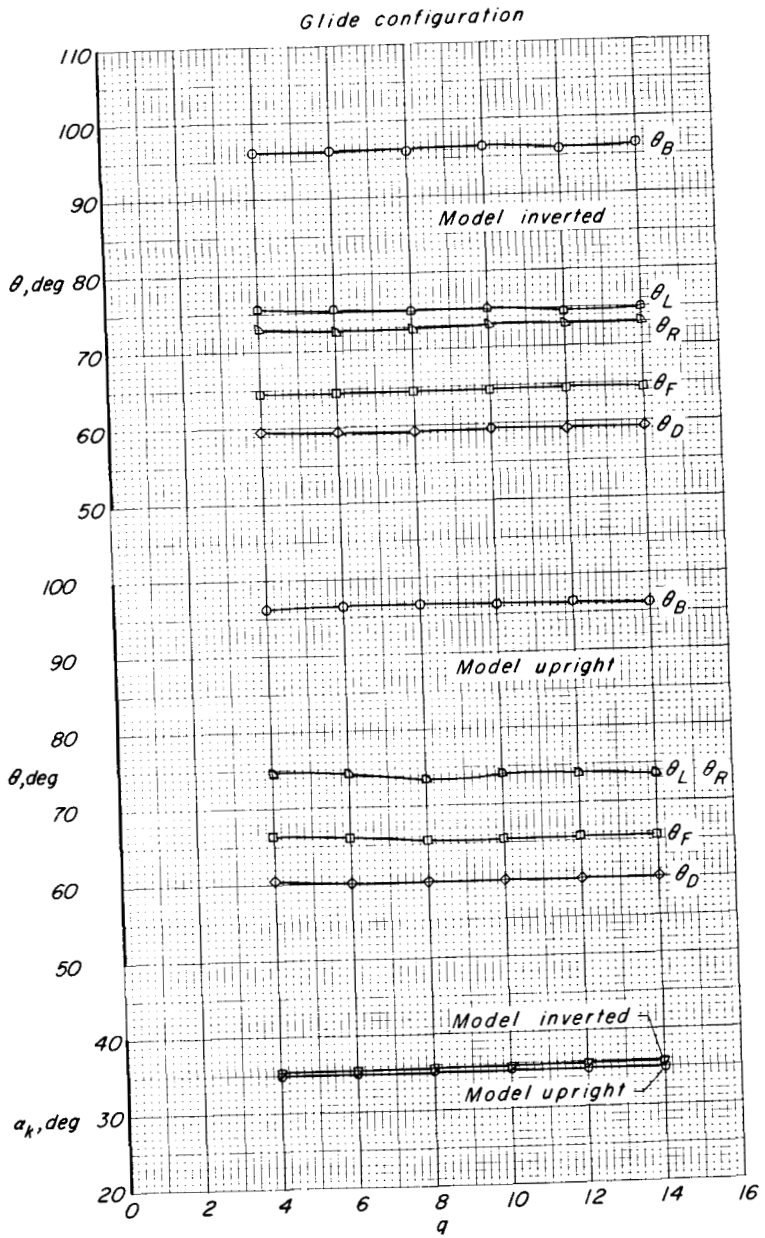

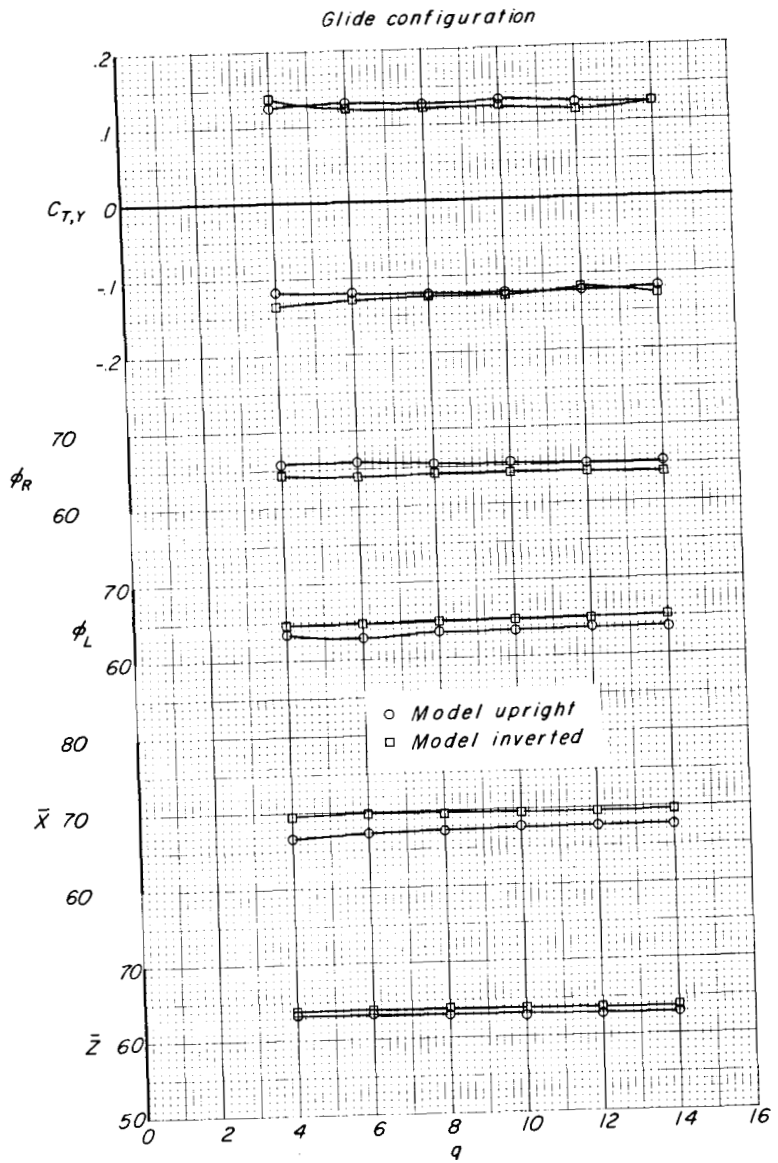

Figure 9.- Concluded.

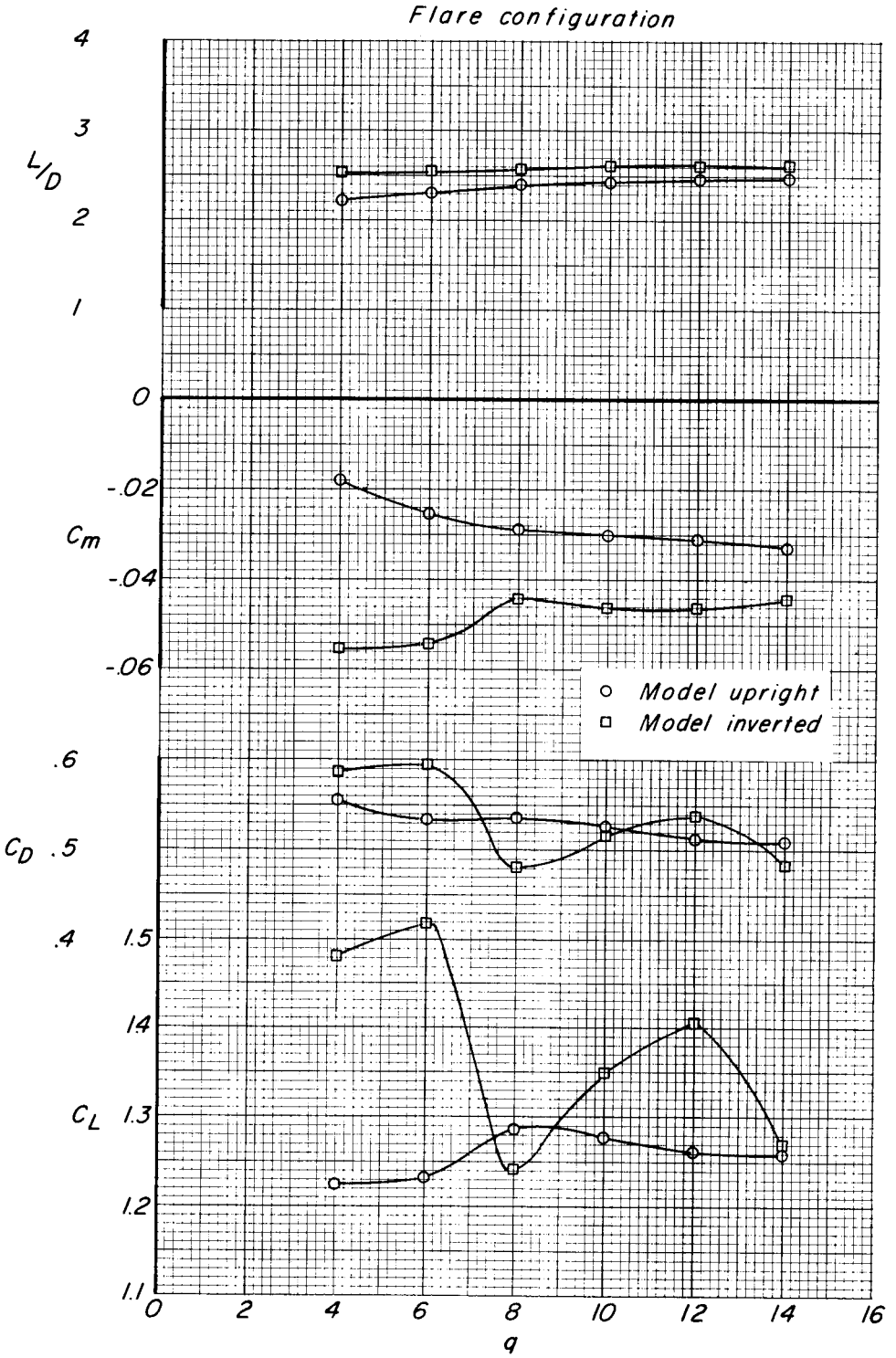

Figure 10.- Comparison of results obtained over a range of dynamic pressure with model upright and inverted for flare configuration. $\alpha = 0^{\circ}$; 4-percent boltrope.

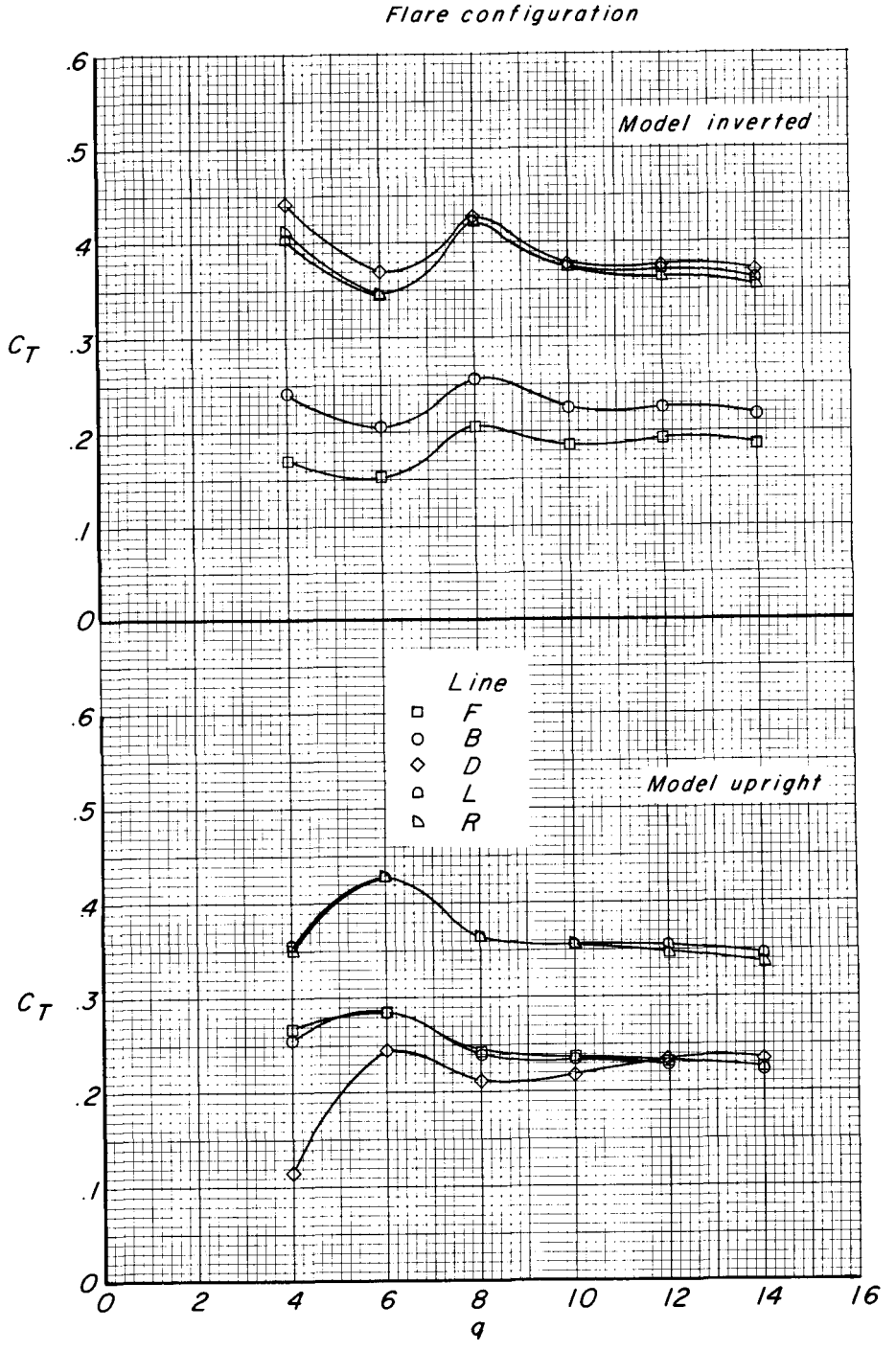

Figure 10.- Continued.

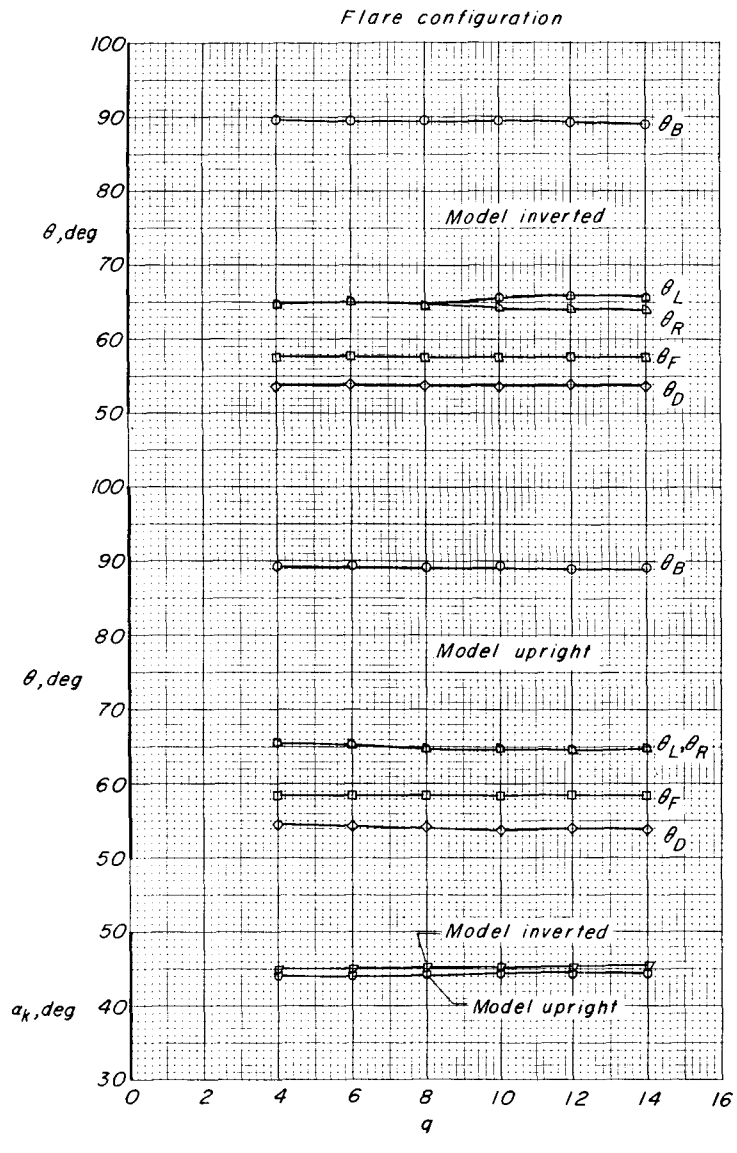

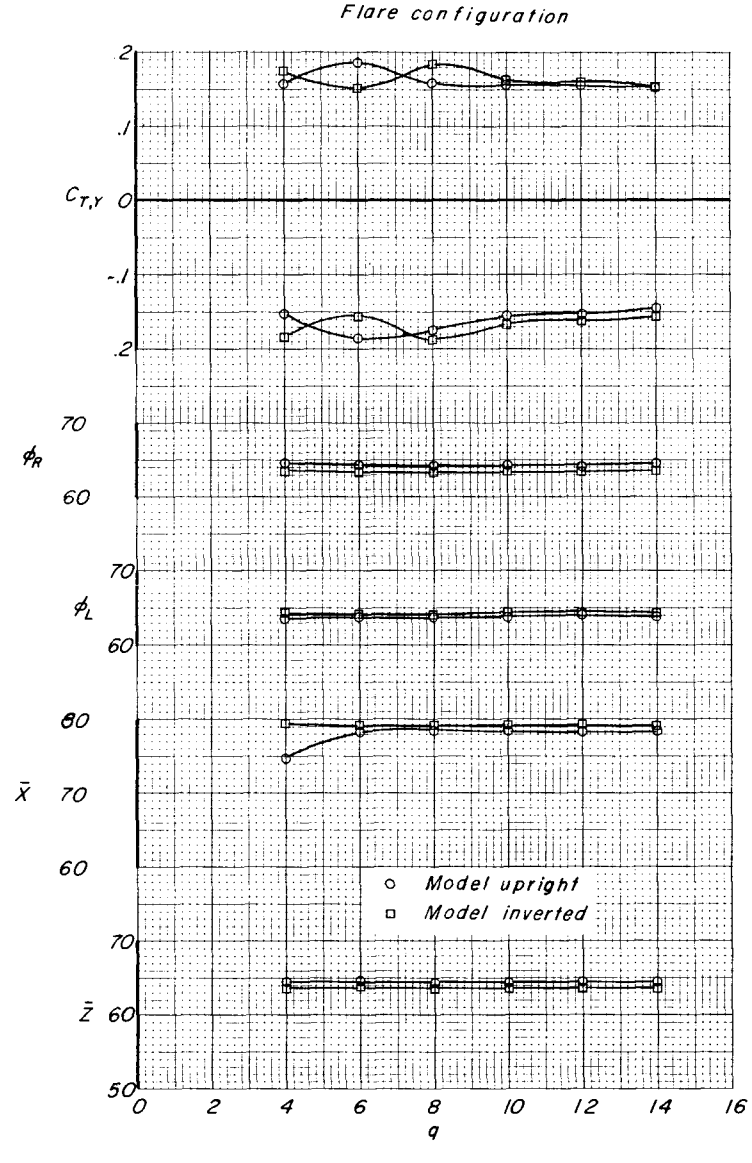

Figure 10.- Concluded.

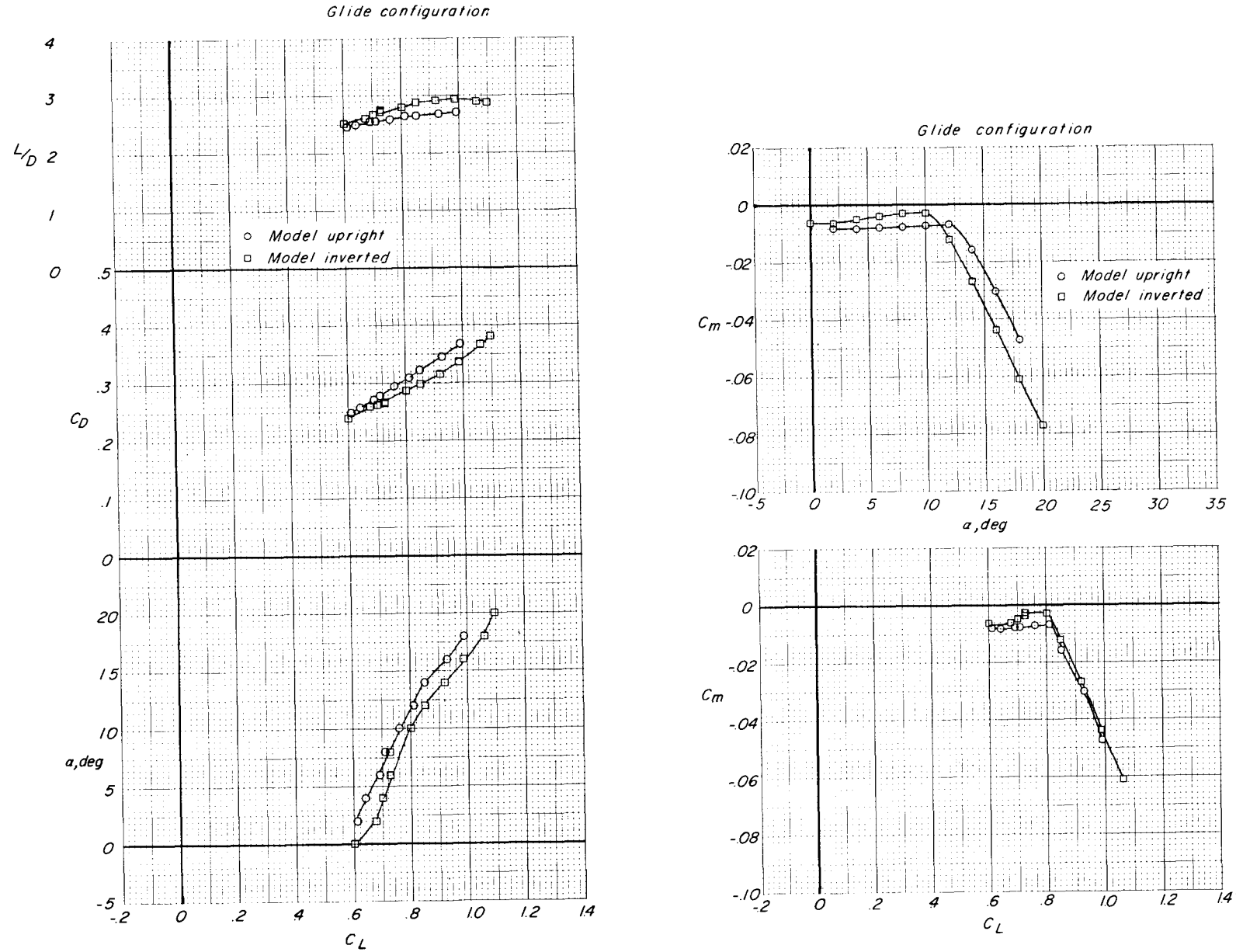

Figure 11.- Comparison of results obtained over range of angle of attack with model upright and inverted for glide configuration. q = 12; 4-percent boltrope.

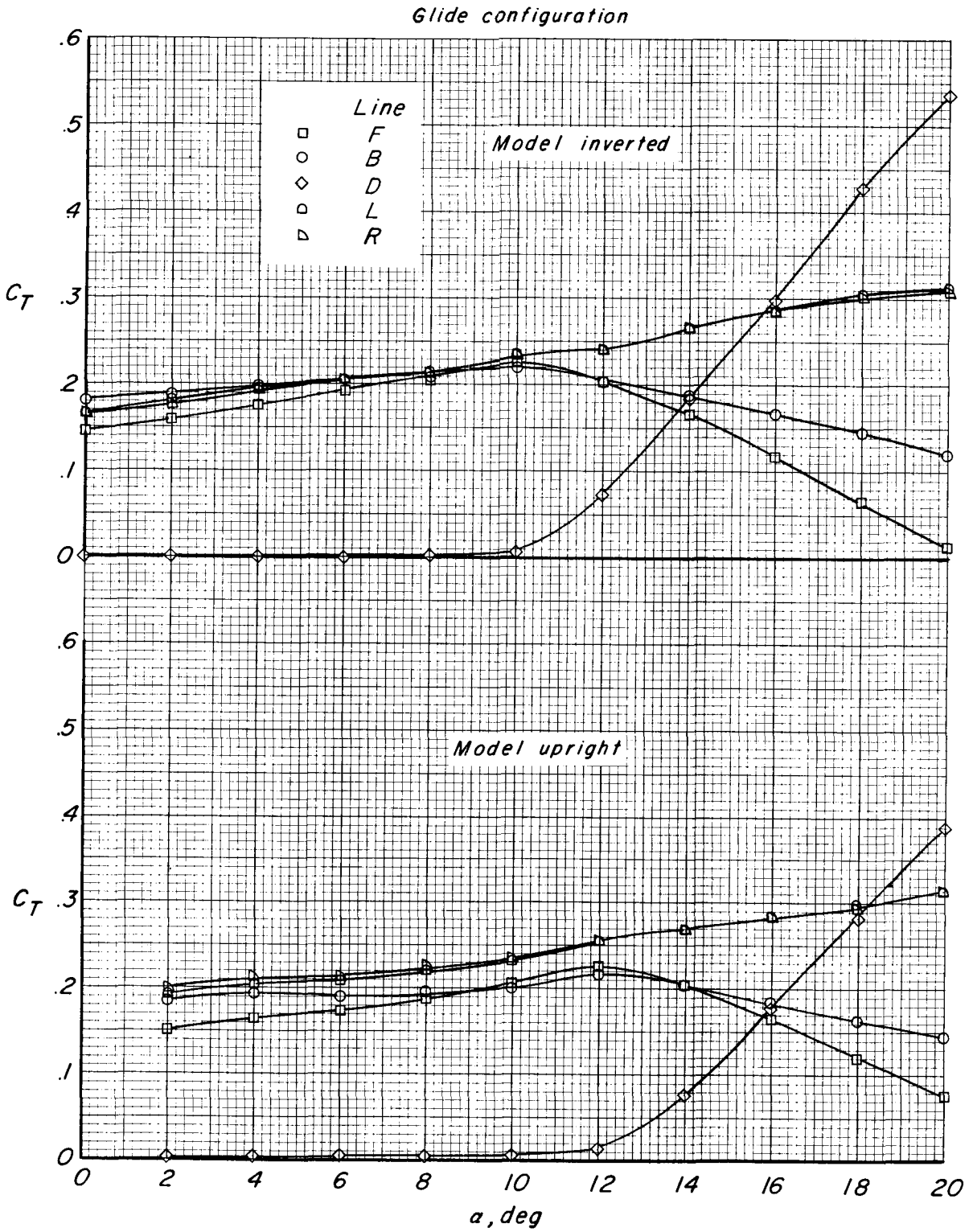

Figure 11.- Continued.

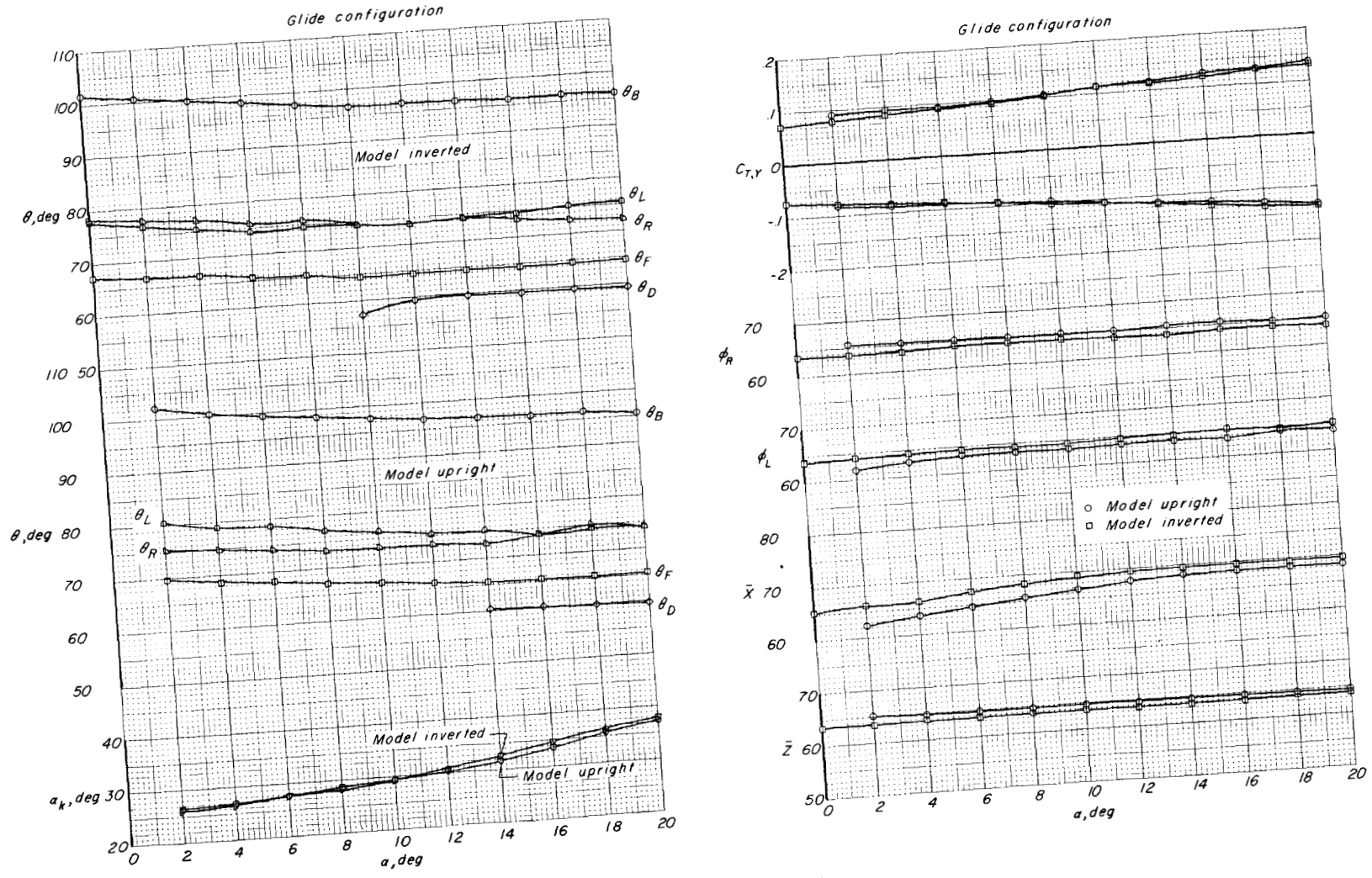

Figure 11.- Concluded.

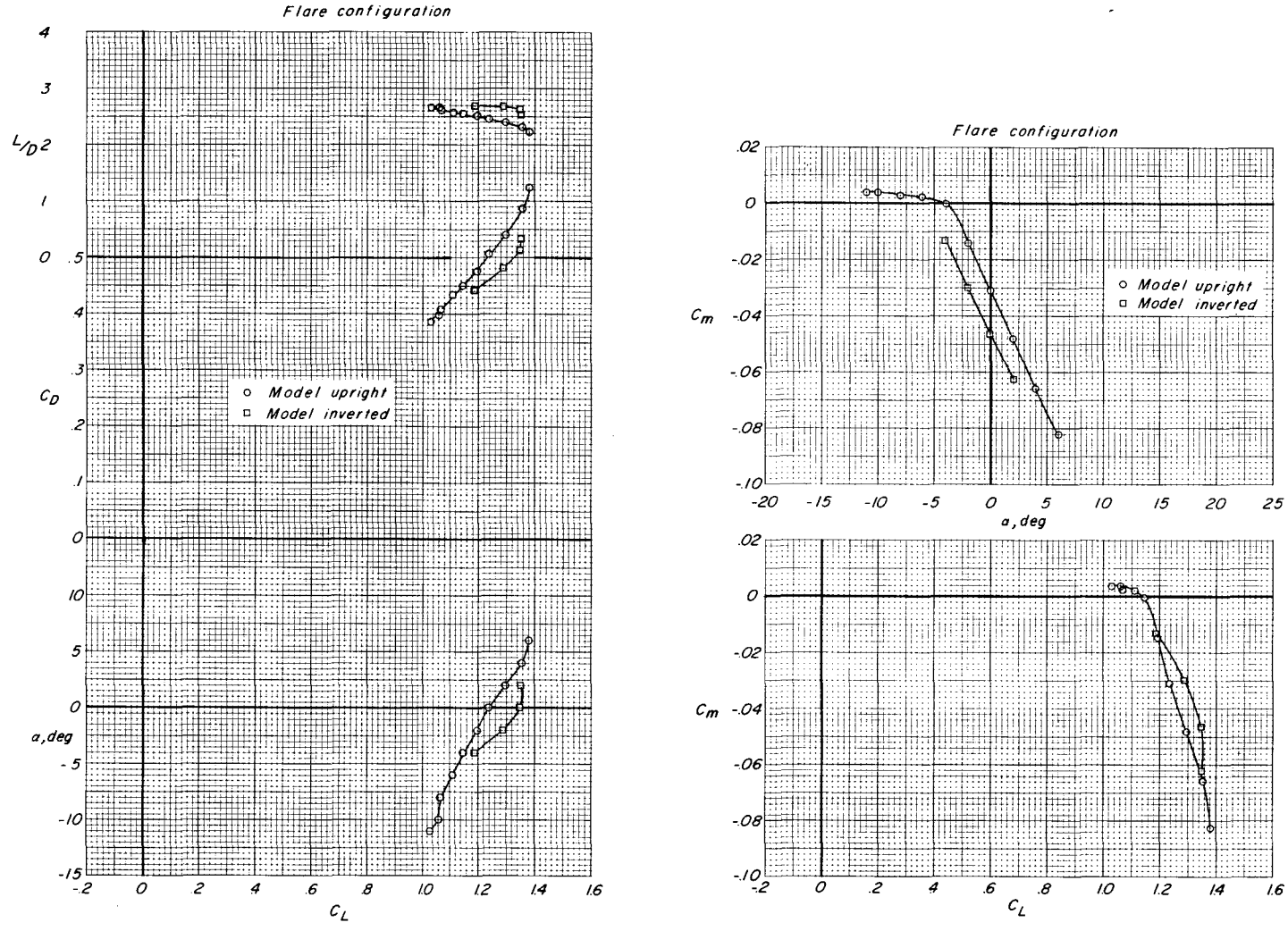

Figure 12.- Comparison of results obtained over range of angle of attack with model upright and inverted for flare configuration. q = 12; 4-percent boltrope.

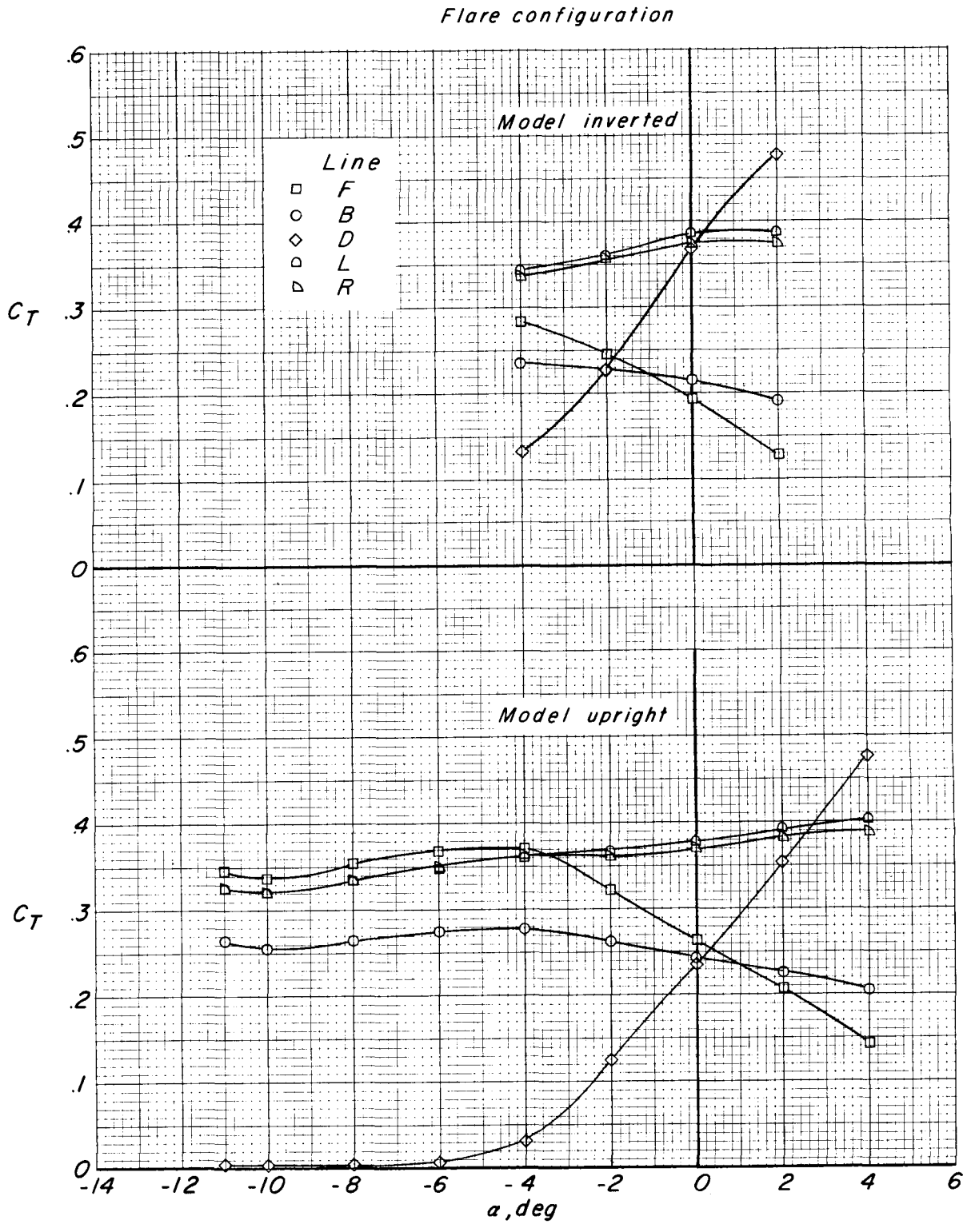

Figure 12.- Continued.

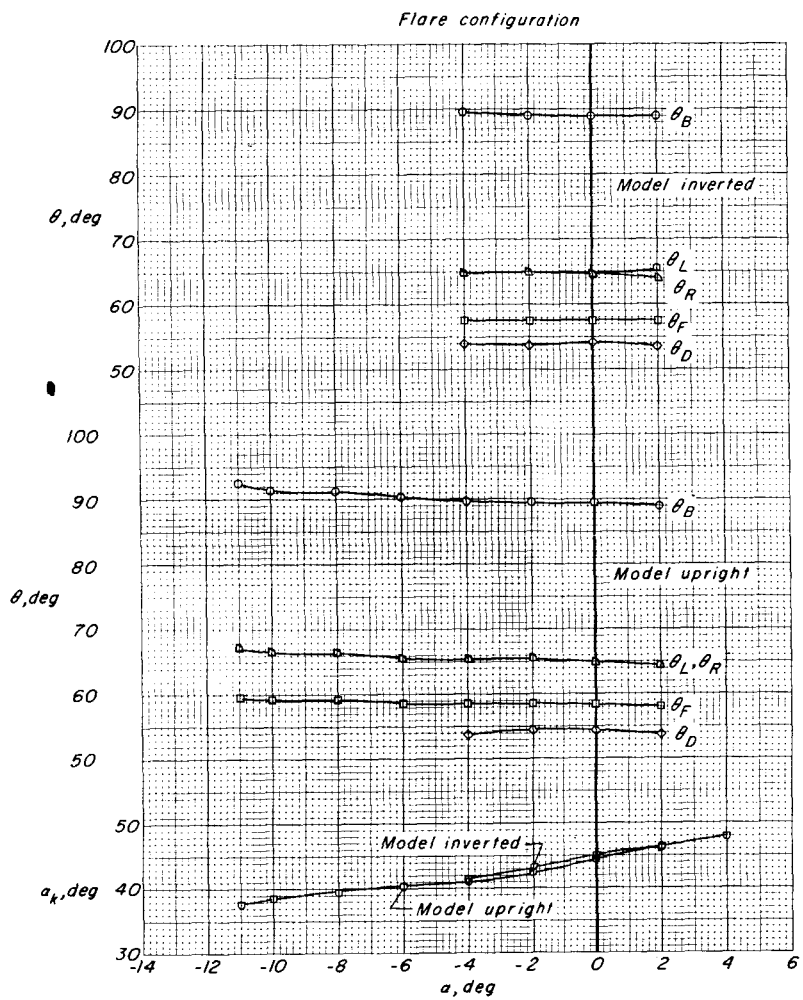

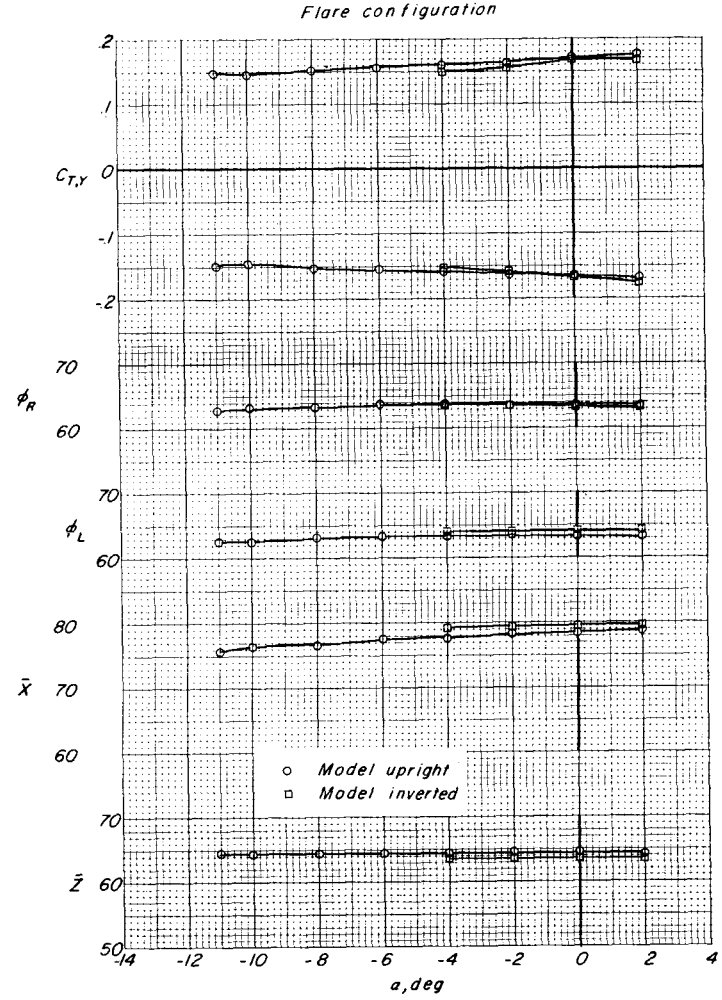

Figure 12.- Concluded.

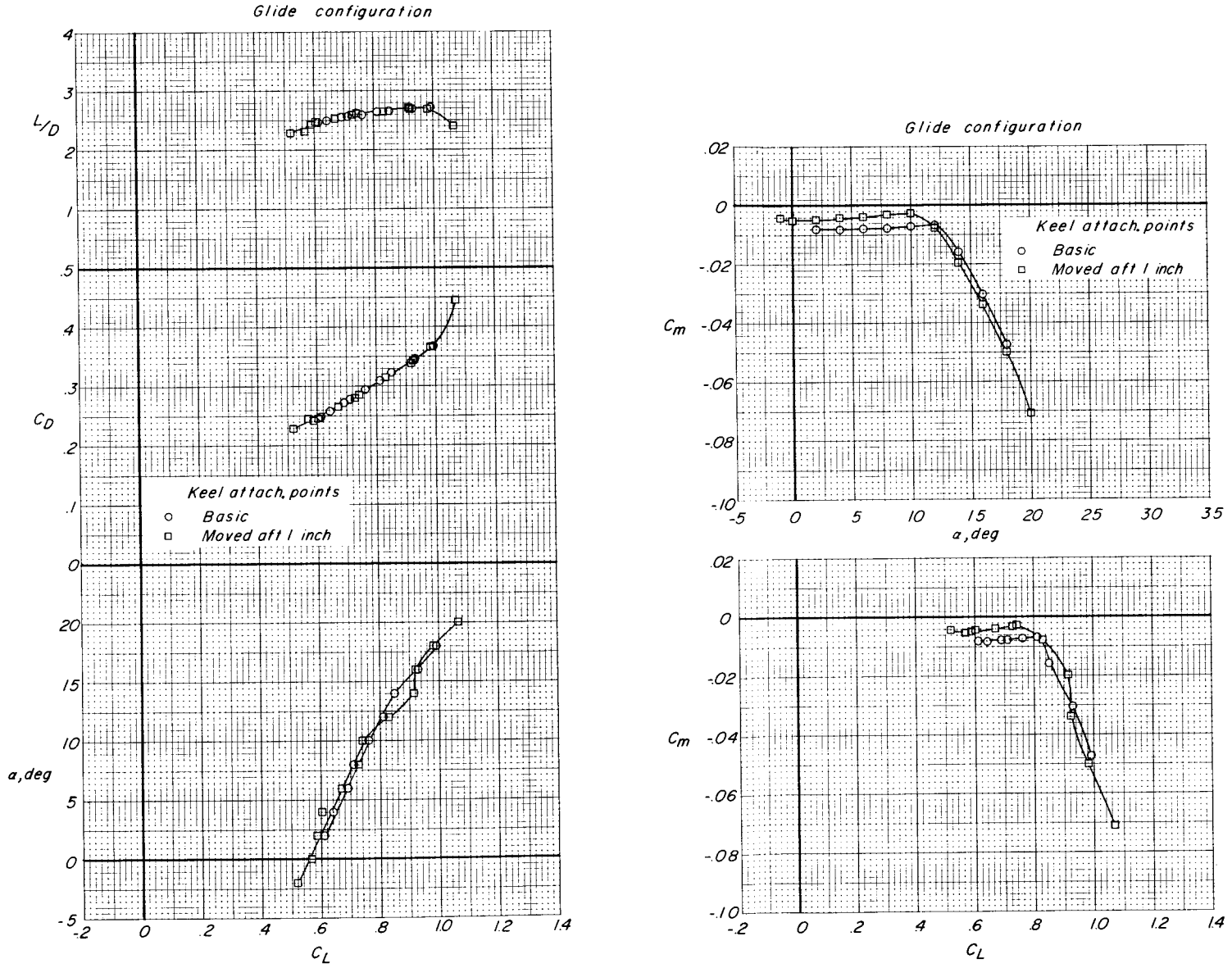

Figure 13.- Effect of moving keel attachment points on aerodynamic characteristics, line loads, and wing position over an angle-of-attack range for glide configuration. q = 12; 4-percent boltrope.

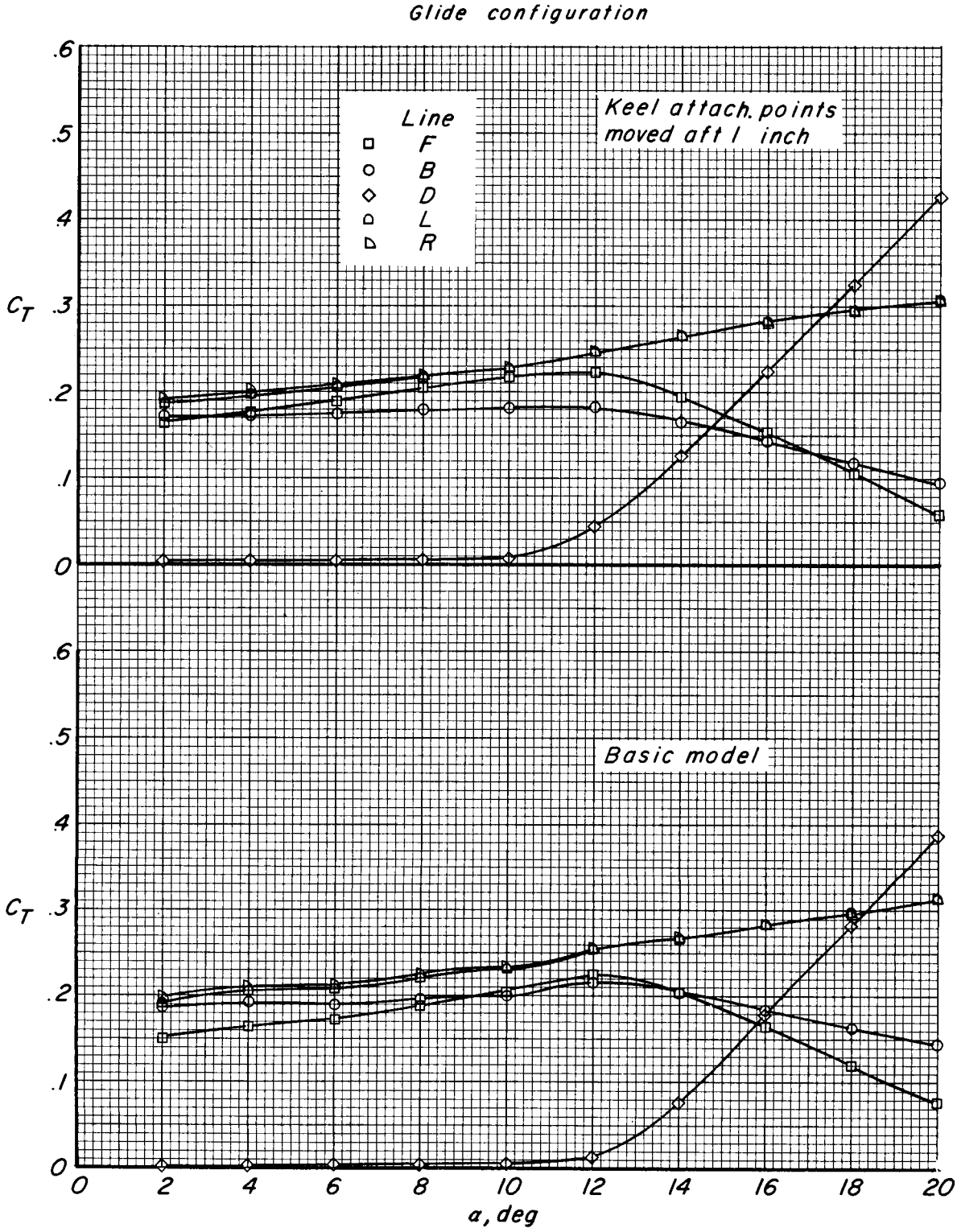

Figure 13.- Continued.

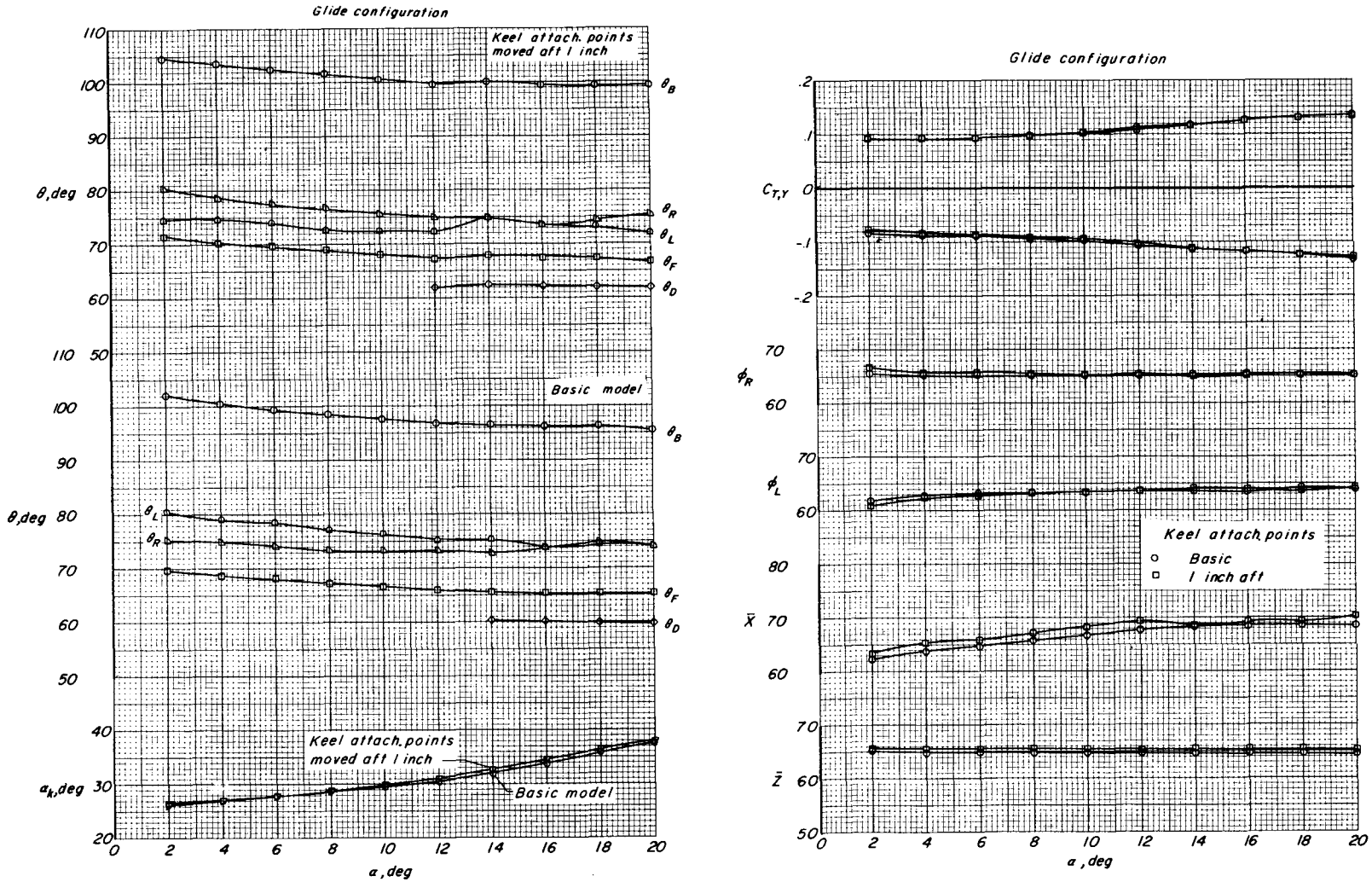

Figure 13.- Concluded.

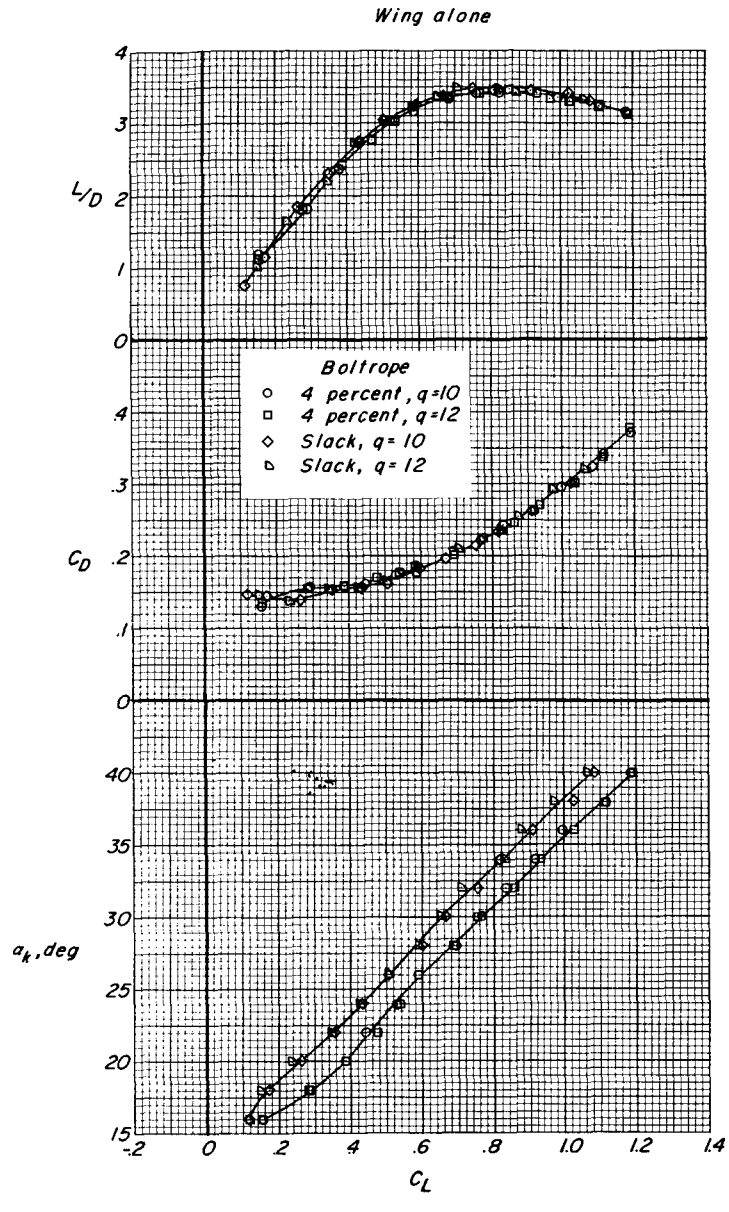

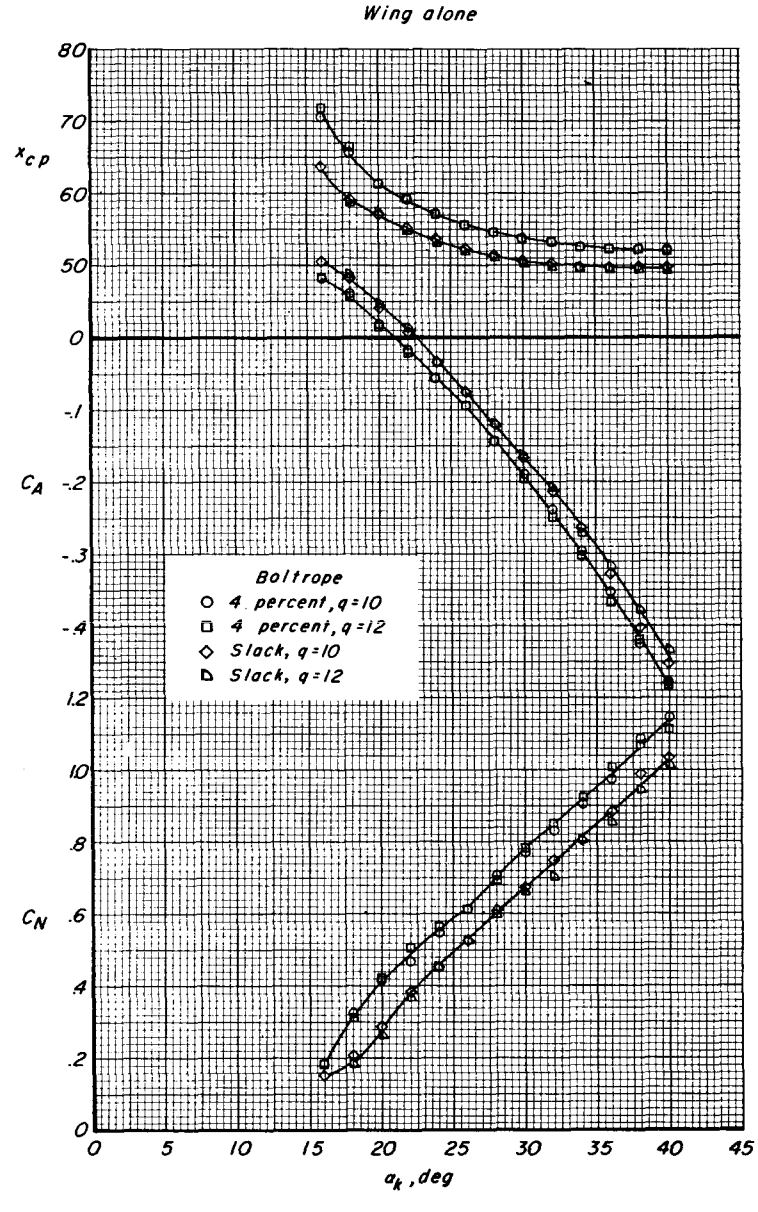

(a) Low angle-of-attack range; $\gamma = 0^{\circ}$.

Figure 14.- Aerodynamic characteristics of wing alone. Moment reference at $0.50l_k$ on keel center line.

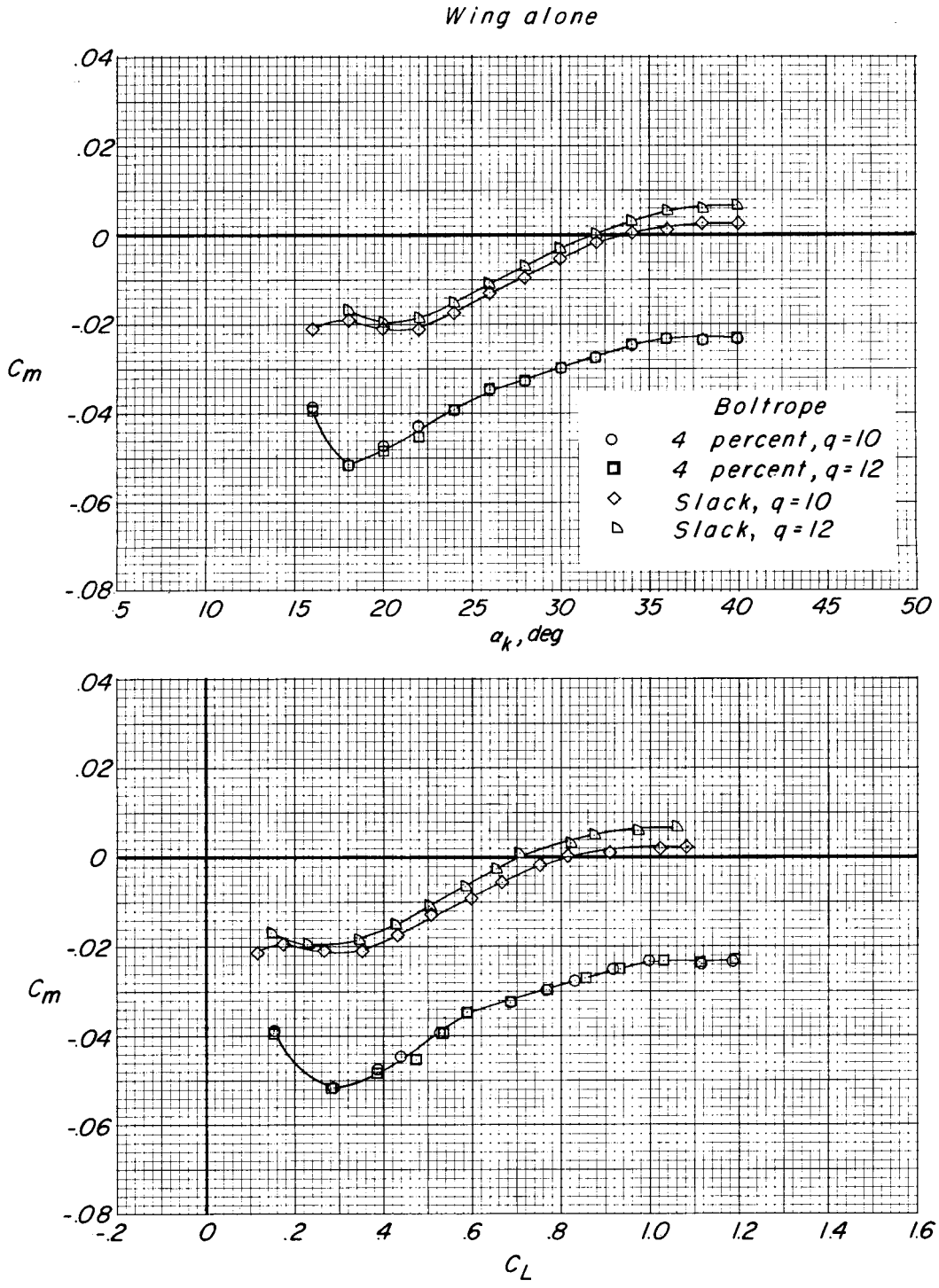

(a) Concluded.

Figure 14.- Continued.

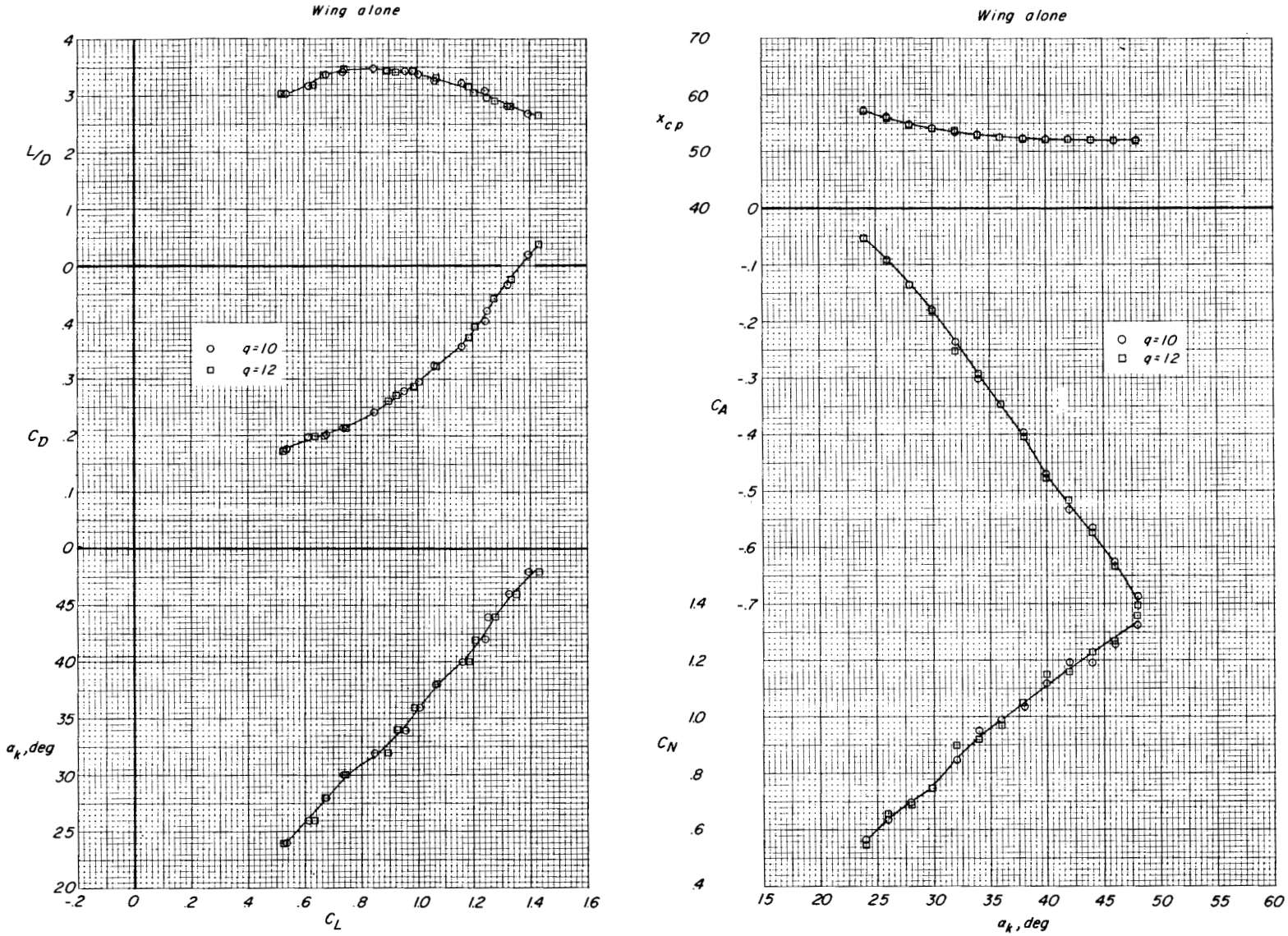

(b) High angle-of-attack range; γ = 7.67°; 4-percent boltrope.

Figure 14.- Continued.

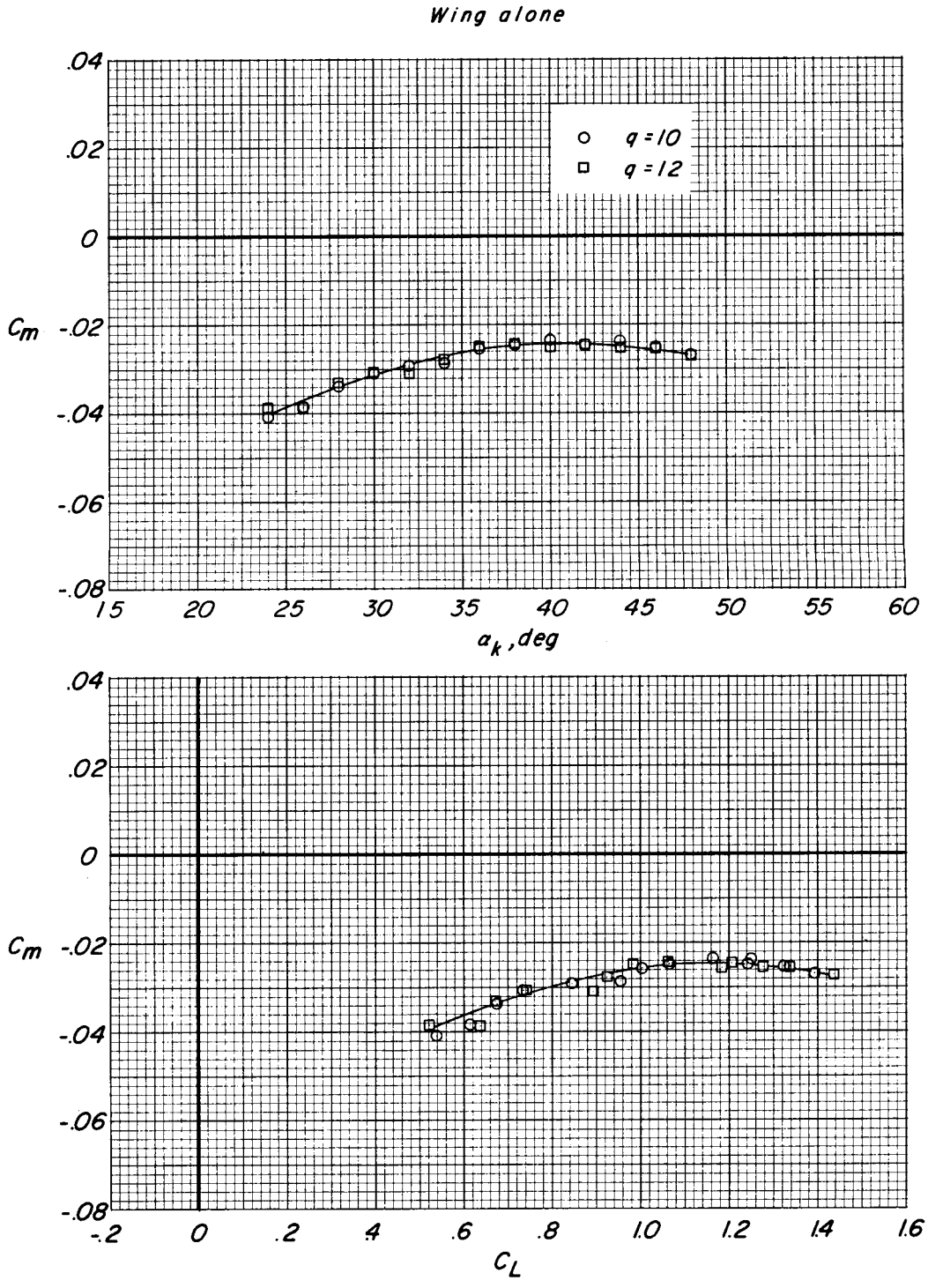

(b) Concluded.

Figure 14.- Concluded.

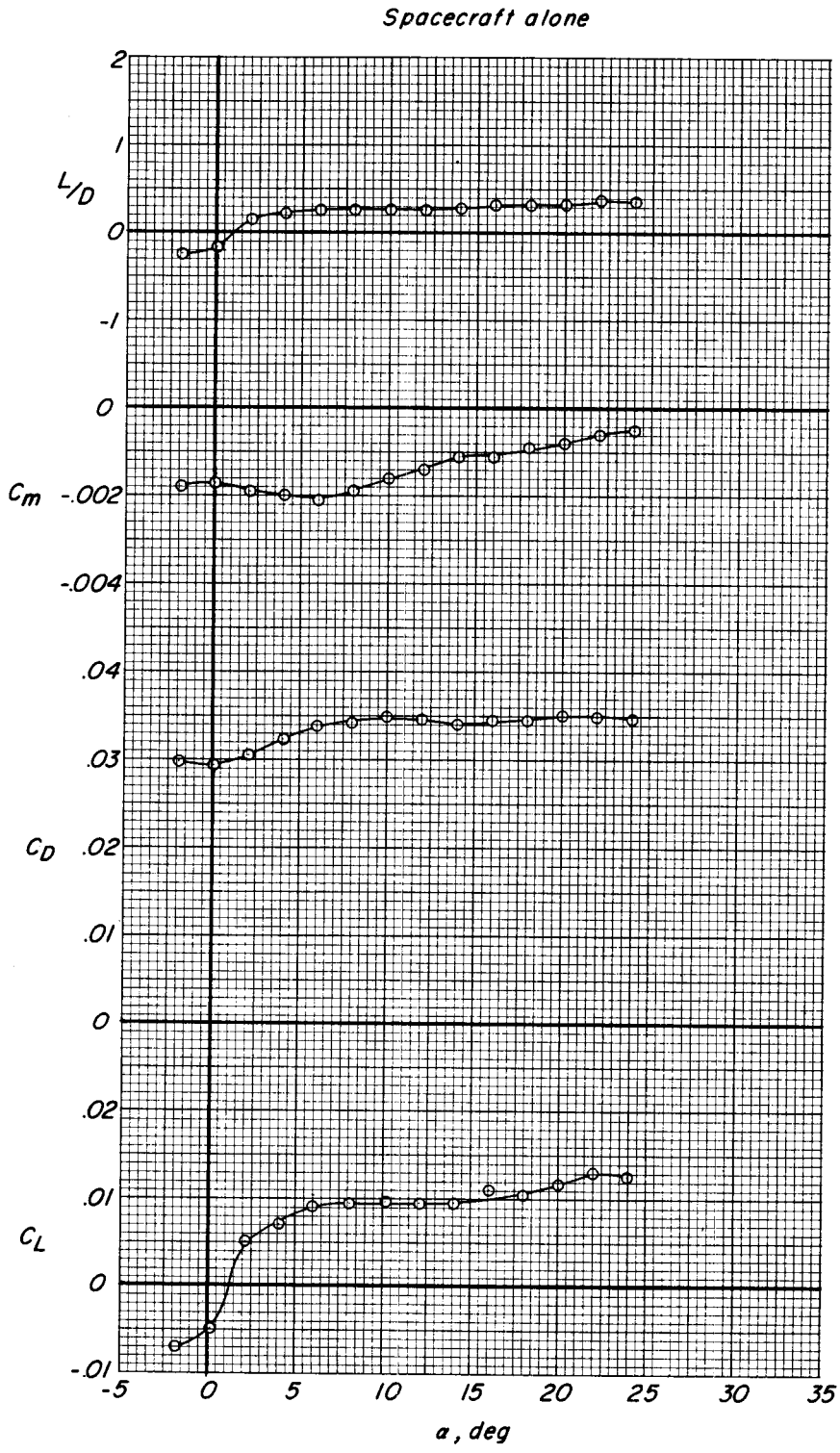

Figure 15.- Aerodynamic characteristics of spacecraft alone. q = 20.

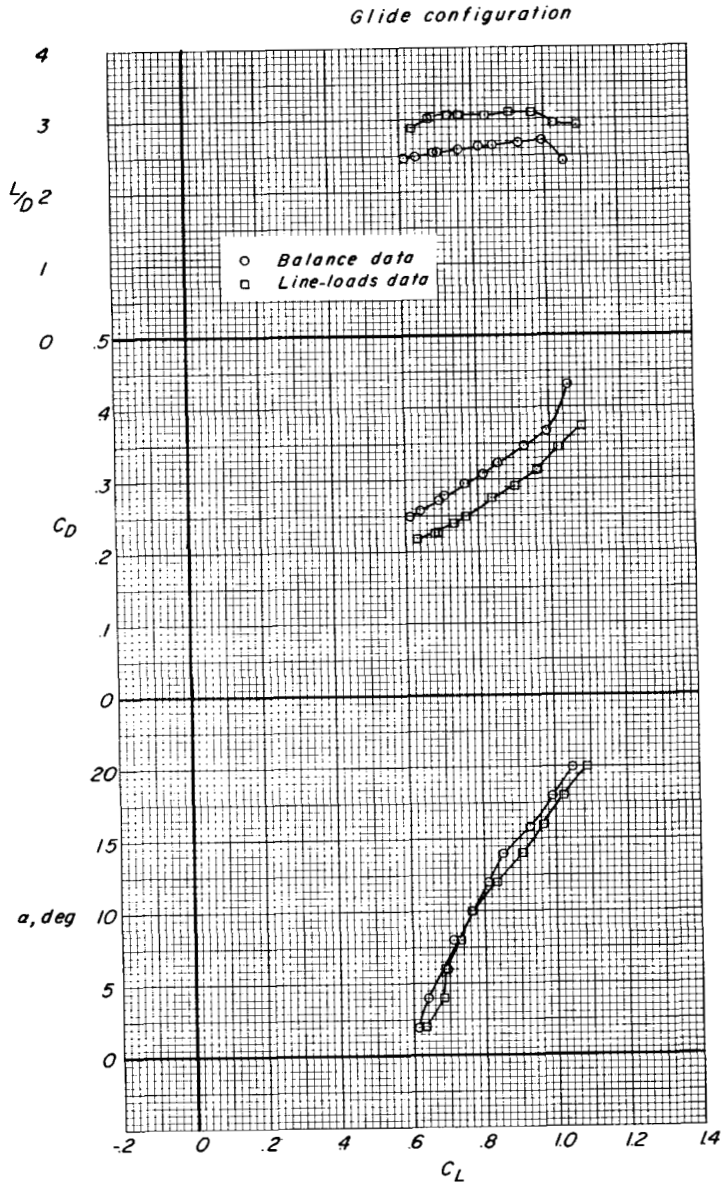

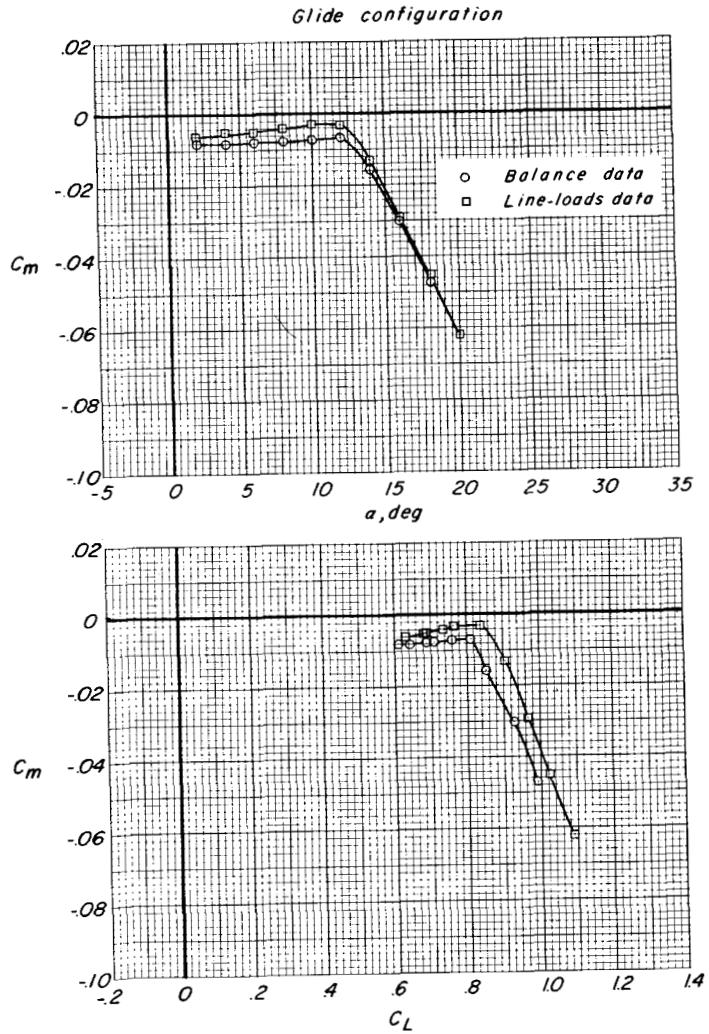

Figure 16.- Comparison of aerodynamic characteristics of glide configuration obtained from internal-balance data and from line-loads data. q = 12; 4-percent boltrope.

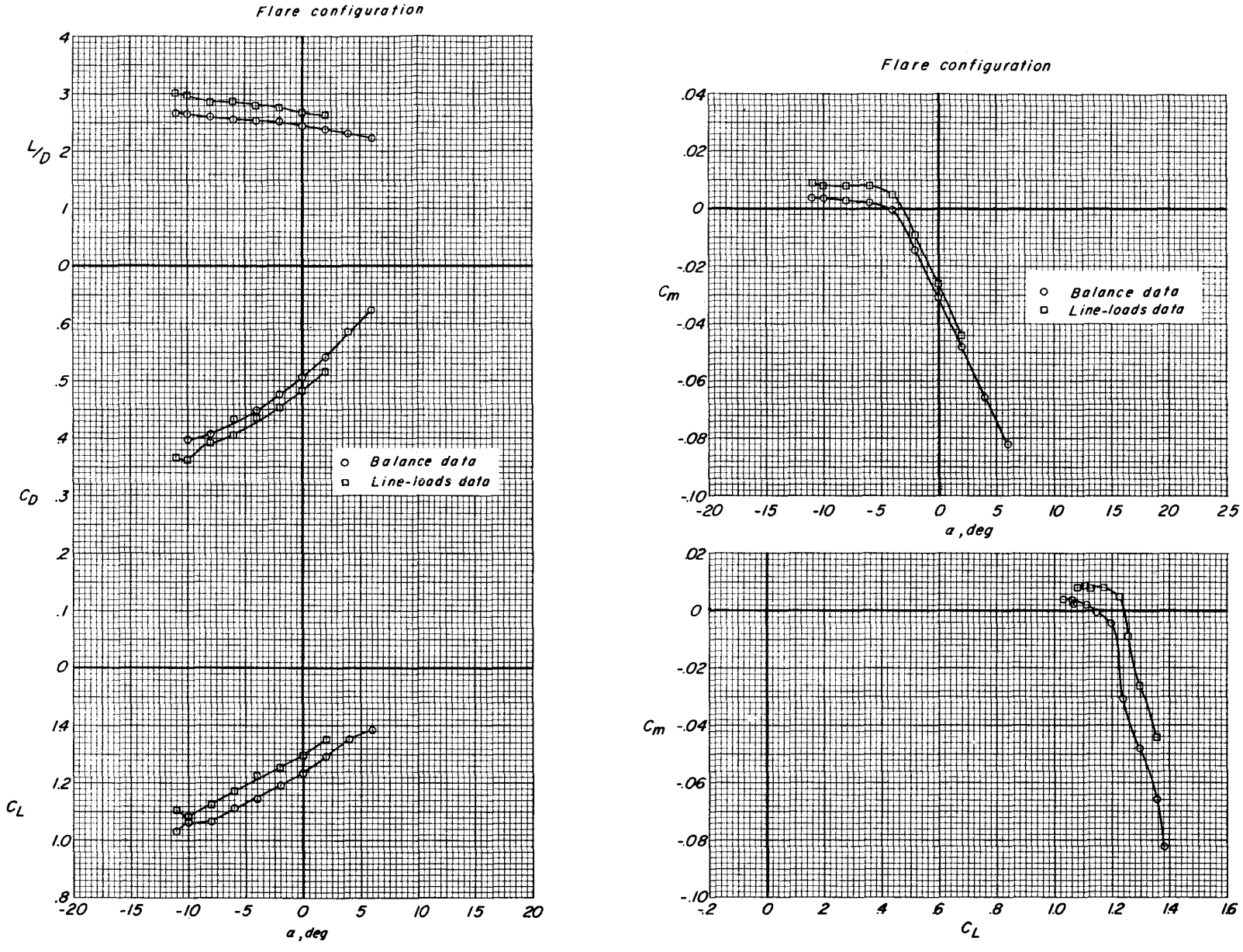

Figure 17.- Comparison of aerodynamic characteristics of flare configuration obtained from internal-balance data and from line-loads data. q = 12; 4-percent boltrope.

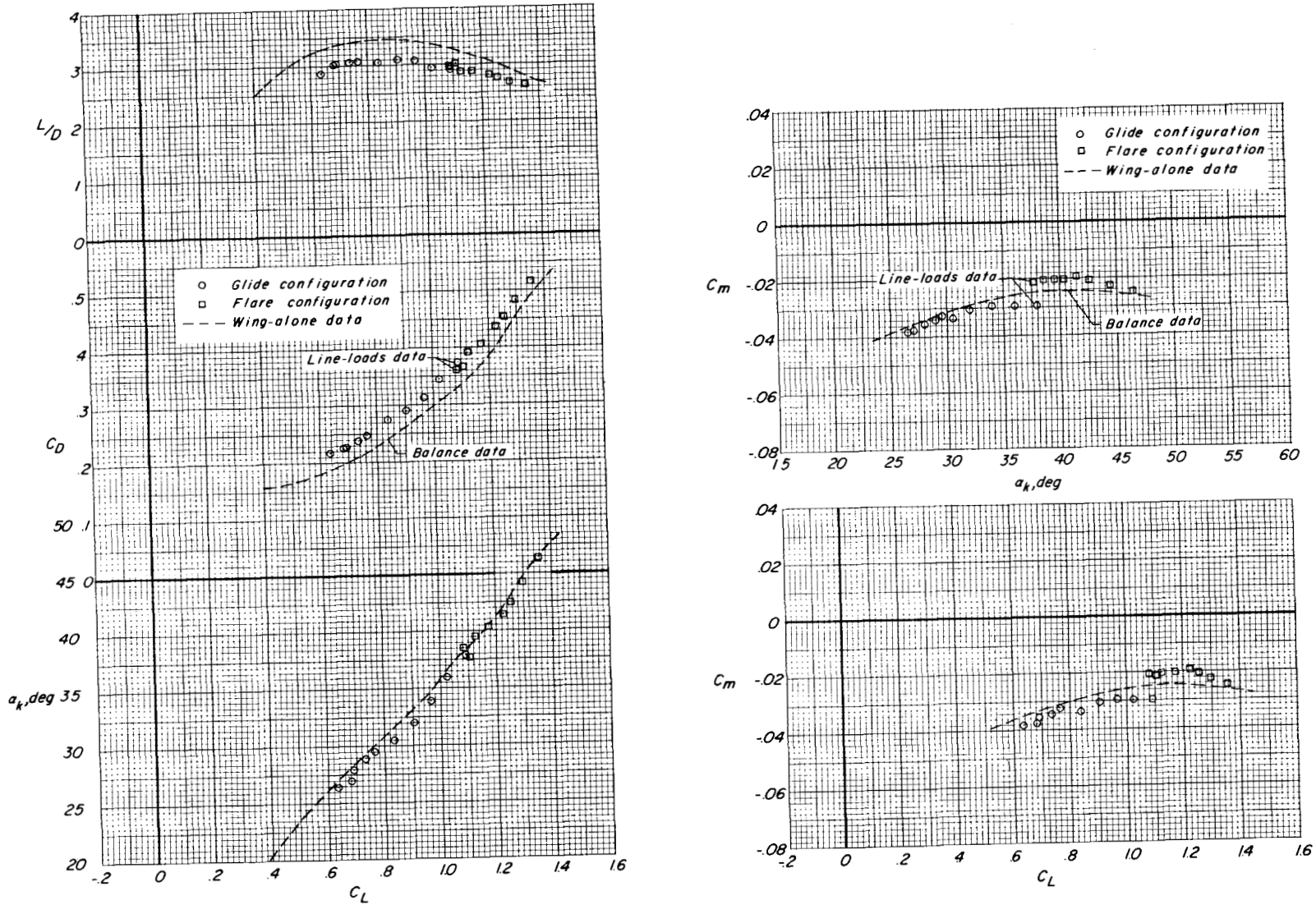

Figure 18.- Comparison of aerodynamic characteristics of wing-alone configuration obtained from internal-balance data and from line-loads data. q = 12; 4-percent boltrope.

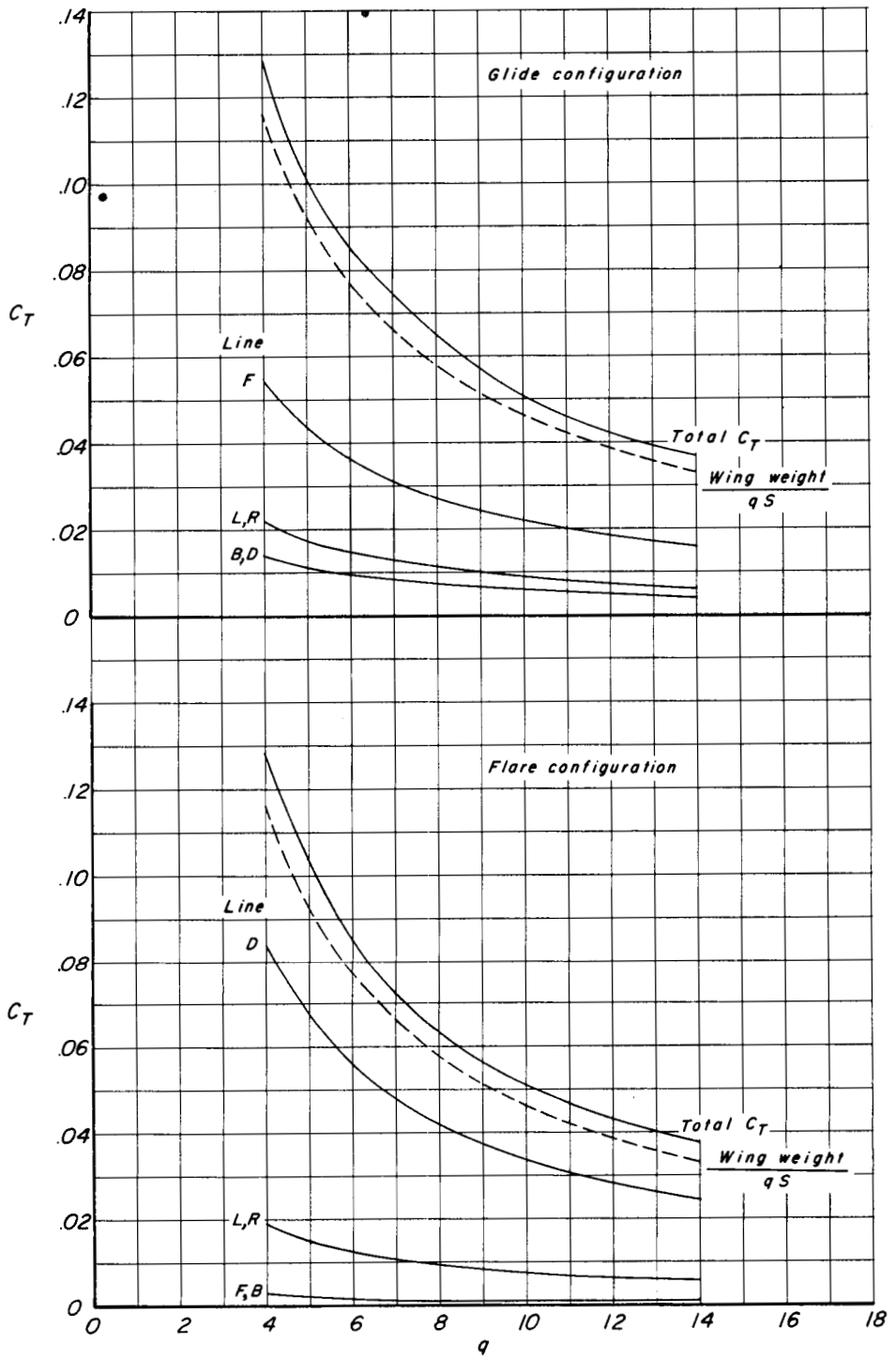

Figure 19.- Wing weight and cable tension obtained with wing hanging from the inverted spacecraft and with the wind off. Weight and tension are expressed in coefficient form for the range of test dynamic pressure investigated.